

DUCTILE FRACTURE STRAIN IN UNIAXIAL TENSILE TEST OF PLANE
SPECIMEN'S

MOHAMED ZULQARNAIN BIN MOHAMED AKRAM

Report submitted in partial fulfillment of the requirements
for the award of the degree of Bachelor of Mechanical Engineering

Faculty of Mechanical Engineering
UNIVERSITI MALAYSIA PAHANG

JUNE 2012

UNIVERSITI MALAYSIA PAHANG

BORANG PENGESAHAN STATUS TESIS [♦]

**JUDUL: DUCTILE FRACTURE STRAIN IN UNIAXIAL TENSILE
TEST OF PLANE SPECIMEN'S**

SESI PENGAJIAN: 2011/2012

Saya, **MOHAMED ZULQARNAIN BIN MOHAMED AKRAM (890422-08-6025)**
(HURUF BESAR)

mengaku membenarkan tesis (Sarjana Muda / ~~Sarjana~~ / ~~Doktor Falsafah~~)* ini disimpan di perpustakaan dengan syarat-syarat kegunaan seperti berikut:

1. Tesis ini adalah hakmilik Universiti Malaysia Pahang (UMP).
2. Perpustakaan dibenarkan membuat salinan untuk tujuan pengajian sahaja.
3. Perpustakaan dibenarkan membuat salinan tesis ini sebagai bahan pertukaran antara institusi pengajian tinggi.
4. **Sila tandakan (√)

SULIT

(Mengandungi maklumat yang berdarjah keselamatan atau kepentingan Malaysia seperti yang termaktub di dalam AKTA RAHSIA RASMI 1972)

TERHAD

(Mengandungi maklumat TERHAD yang telah ditentukan oleh organisasi / badan di mana penyelidikan dijalankan)

TIDAK TERHAD

Disahkan oleh:

(TANDATANGAN PENULIS)

(TANDATANGAN PENYELIA)

Alamat Tetap:

No 13, Lorong Emas,
Taman Darul Ridzuan
36000 Teluk Intan
Perak

NASRUL AZUAN BIN ALANG
(Nama Penyelia)

Tarikh: **25 JUNE 2012**

Tarikh: **25 JUNE 2012**

CATATAN: * Potong yang tidak berkenaan.

** Jika tesis ini SULIT atau TERHAD, sila lampirkan surat daripada pihak berkuasa/organisasi berkenaan dengan menyatakan sekali tempoh tesis ini perlu dikelaskan sebagai SULIT atau TERHAD.

♦ Tesis dimaksudkan sebagai tesis bagi Ijazah Doktor Falsafah dan Sarjana secara Penyelidikan, atau disertasi bagi pengajian secara kerja kursus dan penyelidikan, atau Laporan Projek Sarjana Muda (PSM).

UNIVERSITI MALAYSIA PAHANG
FACULTY OF MECHANICAL ENGINEERING

I certify that the project entitled “*Ductile Fracture Strain In Uniaxial Tensile Test Of Plane Specimen 's*” is written by *Mohamed Zulqarnain Bin Mohamed Akram*. I have examined the final copy of this project and in my opinion; it is fully adequate in terms of scope and quality for the award of degree of Bachelor Engineering. I herewith recommend that it be accepted in partial fulfillment of the requirements for the degree of Bachelor Mechanical Engineering.

MR MOHD FIRDAUS B HASSAN

Examiner

Signature

SUPERVISOR'S DECLARATION

I hereby declare that I have checked this project report and in my opinion this project report is sufficient in terms of scope and quality for the award of the Bachelor of Mechanical Engineering.

Signature :
Name of Supervisor : MR NASRUL AZUAN BIN ALANG
Position : LECTURER
Date : 25 JUNE 2012

STUDENT'S DECLARATION

I declare that this report titled “*DUCTILE FRACTURE STRAIN IN UNIAXIAL TENSILE TEST OF PLANE SPECIMEN'S*” is my result of my own research except as stated in the references. This report has not been accepted for any degree and is not concurrently submitted for award of other degree.

Signature :

Name : MOHAMED ZULQARNAIN BIN MOHAMED AKRAM

Id. Number : MA08112

Date : 25 JUNE 2012

**IN THE NAME OF ALLAH,
THE MOST BENEFICENT, THE MOST MERCIFUL**

*A special dedication of This Grateful Feeling to My
Beloved parents, En.Mohamed Akram Bin Mohammad Ayub and Pn.Asiah Bt. Abdullah
for giving me full of moral and financial support. It is very meaningful to me in order to
finish up my degree's study. Not forgetting also to all my loving brothers and sisters. Last
but not least to all my colleagues and my lovely friends.*

Thanks for all the support, wishes and love.

ACKNOWLEDGEMENT

I am grateful and would like to express my sincere gratitude and deepest appreciation to my supervisor Mr. Nasrul Azuan Bin Alang for his invaluable guidance and constant support in making this thesis. This thesis could not been done without his who not only served as my supervisor but also encourage me throughout the process. I appreciate his consistent support from the first day I applied to graduate program to these concluding moments. I am truly grateful for his progressive vision about my training in science, his tolerance of my naïve mistakes, and his commitment to my future career.

I also would like to express very special thanks to the panel member who give valuable comment and suggestion during my project presentation. My sincere thanks go to all laboratory assistant from Faculty of Mechanical Engineering for their teaching and help during the period of my project.

I acknowledge my sincere indebtedness and gratitude to my parents, Mr. Mohamed Akram Bin Mohammad Ayub and Mdm. Asiah Binti Abdullah for their love and sacrifice throughout my life. They have always supported my dreams. They did a good job raising me to improve myself. Special thanks should be given to my committee members. I would like to acknowledge their comments and suggestions, which was crucial for the successful completion of this study.

ABSTRACT

This project was performed to determine the ductile fracture strain in uniaxial tensile test of plane specimen. In this project, uniaxial tensile test was performed for three different materials that are aluminum, brass and mild steel. The objective of the test is to identify the value of uniaxial fracture strain for these three different materials. The specimens have been divided into three different areas: L, P-lateral and S-middle zones. The zones are measured using optical microscope before and after the tensile test to determine the value of ductile fracture strain at those zones. However, the result from tensile test gives an average value of ductile fracture strain. The second step was to determine the suitable point or area to get the accurate uniaxial ductile fracture strain. The element of the material with stress triaxiality, $k = 0.33$ is the location where the uniaxial fracture strain was occurred. Finite element analysis using MSC Patran/Marc 2008r1 software was used to determine the element with stress triaxiality, $k = 0.33$. In MSC Patran software, the specimen was divided into several nodes to represent the study location for lateral and middle zones. In this project, the model was divided into eleven points. Each point has different values of stress triaxiality after ultimate tensile strength occurred. The finite element analysis data of engineering stress-strain curve was compared with experiment engineering stress-strain curve in order to determine the fracture point of the model. The state of stress for each material was determined in order to get the uniaxial ductile fracture strain nodes. The result shows that uniaxial ductile fracture strain occurred at nodes 2577 for aluminum and brass, while uniaxial ductile fracture strain for mild steel occurred at node 2598. It is also shown that the fracture strain at L and P-lateral zones was the nearest to the uniaxial ductile fracture strain.

ABSTRAK

Projek ini telah dijalankan untuk menentukan terikan patah mulur dalam ujian tegangan ekapaksi spesimen satah. Dalam projek ini, ujian tegangan sepaksi telah dilakukan untuk tiga bahan yang berbeza iaitu aluminium, tembaga dan keluli lembut. Objektif ujian ini adalah untuk mengenal pasti nilai terikan patah unipaksi untuk ketiga-tiga bahan berbeza. Spesimen telah dibahagikan kepada tiga kawasan berbeza: L, P-sisi dan zon S-tengah. Zon diukur dengan menggunakan mikroskop optik sebelum dan selepas ujian tegangan untuk menentukan nilai terikan patah mulur di zon-zon berkenaan. Walau bagaimanapun, hasil daripada ujian tegangan memberikan nilai purata terikan patah mulur. Langkah kedua adalah untuk menentukan titik atau kawasan yang sesuai untuk mendapatkan nilai patah yang tepat berketegangan mulur ekapaksi. Unsur bahan dengan triaxiality tegasan, $k = 0.33$ adalah lokasi di mana terikan patah ekapaksi telah berlaku. Analisis unsur terhingga menggunakan perisian MSC Patran / Marc 2008r telah digunakan untuk menentukan elemen dengan triaxiality tegasan, $k = 0.33$. Dalam perisian MSC Patran, spesimen telah dibahagikan kepada beberapa nod mewakili lokasi kajian untuk zon sisi dan sederhana. Dalam projek ini, model itu dibahagikan kepada 11 titik. Setiap titik mempunyai perbezaan nilai triaxiality tegasan selepas kekuatan tegangan muktamad berlaku. Analisis terhingga data unsur lengkung kejuruteraan tegasan-terikan berbanding dengan eksperimen kejuruteraan lengkung tegasan-terikan untuk menentukan titik patah model. Keadaan tegasan bagi setiap bahan yang telah ditentukan untuk mendapatkan terikan ekapaksi nod patah mulur. Hasilnya menunjukkan bahawa ketegangan patah mulur ekapaksi yang berlaku pada nod 2577 untuk aluminium dan tembaga, manakala terikan patah mulur ekapaksi untuk keluli lembut berlaku pada nod 2598. Ia juga menunjukkan bahawa terikan patah di zon L dan P hala adalah yang terdekat untuk terikan patah mulur ekapaksi.

TABLE OF CONTENTS

	Page
SUPERVISOR’S DECLARATION	ii
STUDENT’S DECLARATION	iii
DEDICATION	iv
ACKNOWLEDGEMENT	v
ABSTRACT	vi
ABSTRAK	vii
TABLE OF CONTENTS	viii
LIST OF TABLES	xi
LIST OF FIGURES	xii
LIST OF SYMBOLS	xvi
LIST OF ABBREVIATIONS	xvii

CHAPTER 1 INTRODUCTION

1.1	Research Background	1
1.2	Problem Statement	2
1.3	Objectives	3
1.4	Scopes Of Study	3

CHAPTER 2 LITERATURE REVIEW

2.1	Introduction	4
2.2	Experimental Test Setup	4
2.3	Wire-Cut EDM Review	7
2.4	Engineering Stress-Strain Curve	8
2.5	True Stress-Strain Curve	11

2.6	Finite Element Analysis (FEA) Simulation	15
2.7	Stress Triaxiality And Ductile Fracture Strain	19

CHAPTER 3 METHODOLOGY

3.1	Introduction	23
3.2	Research Flow Chart	23
3.3	Specimen Preparation	25
	3.3.1 Specimen Specification	25
	3.3.2 Machining Process	26
	3.3.3 Polishing Process	30
	3.3.4 Zone Marking Process	31
3.4	Tensile Test	34
3.5	Measurement Of Zone Length	37
3.6	Finite Element Analysis (FEA)	39
	3.6.1 Modeling, Meshing and Solving Process	40

CHAPTER 4 RESULT AND DISCUSSION

4.1	Introduction	52
4.2	Experiment Result	52
	4.2.1 Engineering Stress-Strain Graph	53
	4.2.2 Conversion of Engineering Stress-Strain Curve To True Stress-Strain Curve	56
	4.2.3 The Result For Every Zone	60
4.3	Finite Element Analysis (FEA) Result	64
4.4	Ductile Fracture Strain	73
4.5	Stress Triaxiality	78

CHAPTER 5 CONCLUSION AND RECOMMENDATION

5.1	Conclusion	85
5.2	Recommendation	86

REFERENCES	87
-------------------	----

APPENDICES

Appendix A	89
Appendix B	90
Appendix C	91
Appendix D	92
Appendix E	93
Appendix F	94

LIST OF TABLES

Table No.		Page
2.1	Chemical composition of BV-DH32 steel	6
2.2	Typical mechanical properties of BV-DH32 steel	6
2.3	Breadth and thickness in reduced section	6
2.4	Measured mechanical properties of BV Grade DH32 steel	20
2.5	Comparison of equivalent strain to fracture of dog-bone specimen between simulations and test of dog-bone specimens	21
3.1	The direction of polishing process for difference sandpaper grit number	30
3.2	The value of young modulus and poisson ratio for each material used	45
4.1	Mechanical properties of Aluminum obtained from tensile test	54
4.2	Mechanical properties of Brass obtained from tensile test	55
4.3	Mechanical properties of Mild steel obtained from tensile test	56
4.4	Mechanical properties of material tested	59
4.5	Experimental result for ductile fracture strain	62
4.6	Specimen's geometry and average strain values in analyzed regions	63
4.7	The stress triaxiality at every node for aluminum specimen	79
4.8	The stress triaxiality at every node for brass specimen	81
4.9	The stress triaxiality at every node for mild steel specimen	82
4.10	Ductile fracture strain for aluminum at different zones	84
4.11	Ductile fracture strain for brass at different zones	84
4.12	Ductile fracture strain for mild steel at different zones	84

LIST OF FIGURES

Figure No.		Page
1.1	Cross-sectional area in the neck at fracture: a) before fracture, and b) after fracture	2
2.1	A photo of test set up for specimen P34	7
2.2	Engineering stress strain curve for a typical engineering alloy	9
2.3	Comparison of engineering and true stress-strain curves	10
2.4	Typical stress-strain curve	12
2.5	Example of true stress-strain plot	14
2.6	Stress triaxiality, k for an individual plane stress cases: a) biaxial compression, b) uniaxial compression, c) simple shear d) uniaxial tension e) biaxial tension	17
2.7	Comparison of stress triaxiality in different specimen zone: L, P – lateral, S – middle	17
2.8	Shape of plane specimen at fracture point obtained from Finite Element Analysis (FEA)	18
2.9	The moving grids in local necking zone: a) $\epsilon_p = 0.41$, and b) $\epsilon_p = 1.42$ (close to fracture)	19
2.10	The evolution of stress triaxiality calculated by ADINA	22
3.1	Research flow chart	24
3.2	The standard ASTM tensile test dimension for plane specimen	26
3.3	The wire use to cut the material in wire cut machine	27
3.4	Wire cut machine: a) water is use as dielectric liquid, b) wire rotating area	28
3.5	The software use to generate wire cut machine	29
3.6	The straight line from wire cut drawing for first step of cutting the specimen	29

3.7	The second step of drawing that use in cutting material to get tensile specimen	30
3.8	The surface finish after polishing using sandpaper	31
3.9	The highlight region at gauge length	32
3.10	The marking zone with three zone: a) lateral-zone L and P, b) middle-zone S	33
3.11	The marking zone for aluminum specimen	33
3.12	Example of marking zone at tensile specimen	34
3.13	The specimen condition after break for aluminum	35
3.14	The specimen condition after break for brass	35
3.15	The specimen condition after break for mild steel	36
3.16	The specimen break during tensile test	36
3.17	The position of specimen when using microscope	37
3.18	The position of dial gauge when during measurement	38
3.19	The measurement process by using microscope and dial gauge	38
3.20	Distribution of stress triaxiality k: a) Initial phase of tensile test, and b) Final phase of tensile test	40
3.21	Step in PATRAN software	41
3.22	The setting for create a point coordinate	41
3.23	The step in GEOMETRY part from: a) point coordinate, b) make line to combine the point, c) make surface, d) change surface direction	42
3.24	The solid part of the specimen in quarter shape	42
3.25	Step for ELEMENT part: a) mesh seed process, b) the meshing process and c) equivalence process	43
3.26	Step to create boundary condition at the specimen	44
3.27	The FIELD part input data	44
3.28	The PROPERTIES part to change the option into reduced integration	46
3.29	Input properties part	46

3.30	Input data for application region	47
3.31	The analysis part in PATRAN software	48
3.32	The step in job parameter part	48
3.33	Step in load step creation part to set the load increment parameter	49
3.34	Step in load step creation part to set the iteration parameter	49
3.35	The step for load step selection	50
3.36	The step to read the result	50
4.1	Stress versus strain curve for aluminum	53
4.2	Stress versus strain curve for brass	54
4.3	Stress versus strain curve for mild steel	55
4.4	True plastic stress-strain curve for aluminum	57
4.5	True plastic stress-strain curve for brass	58
4.6	True plastic stress-strain curve for mild steel	58
4.7	Failed specimen for all material. From left are aluminum, mild steel and brass	60
4.8	Typical tensile specimen for flat specimen	61
4.9	The elongation of aluminum in finite element analysis	64
4.10	The simulation result for aluminum in 3D view	65
4.11	The shape of saddle at the break point for aluminum	67
4.12	The elongation of brass in finite element analysis	67
4.13	The simulation result for brass in 3D view	67
4.14	The shape of saddle at the break point for brass	68
4.15	The elongation of mild steel in finite element analysis	69
4.16	The simulation result for mild steel in 3D view	70
4.17	The shape of saddle at the break point for mild steel	70
4.18	The comparison of engineering stress-strain data obtained from finite element analysis for different materials	72
4.19	Comparison of stress-strain curve between experiment data and finite element result for aluminum	74

4.20	Comparison of stress-strain curve between experiment data and finite element result for brass	75
4.21	Comparison of stress-strain curve between experiment data and finite element result for mild steel.	76
4.22	Study nodes location in Finite Element Analysis (FEA)	77
4.23	The comparison of stress triaxiality for aluminum in different zones: <i>L</i> , <i>P</i> -lateral, <i>S</i> -middle and all study nodes	78
4.24	The comparison of stress triaxiality for brass in different zones: <i>L</i> , <i>P</i> -lateral, <i>S</i> -middle and all study nodes	80
4.25	The comparison of stress triaxiality for mild steel in different zones: <i>L</i> , <i>P</i> -lateral, <i>S</i> -middle and all study nodes	81

LIST OF SYMBOLS

k	Stress triaxiality
b_0	Breadth length
t_0	Thickness length
σ	Stress, MPa
ε	Strain
$\sigma_{uts} = \sigma_u$	Ultimate tensile strength, MPa
$\sigma_{0.2\%YS} = \sigma_y$	0.2% offset yield strength, MPa
E	Young modulus
A_0	Cross-sectional area
L_0	Length
P	Pressure
ΔL	Total length
K	Strain hardening coefficient
n	Strain hardening exponent
σ_m	Mean normal stress, MPa
σ_H	Equivalent stress, MPa
$\varepsilon_p = \varepsilon_f$	Fracture strain
b_0	Width of specimen before test
b_1	Width of specimen after test
g_0	Length of specimen before test
g_1	Length of specimen after test
$\varepsilon_1 = \varepsilon_2 = \varepsilon_p$	Plastic strain
F	Force, N
σ_E	Engineering stress
σ_T	True stress
ε_E	Engineering strain
ε_T	True strain

LIST OF ABBREVIATIONS

FEA	Finite Element Analysis
ASTM	American Society for Testing and Materials
UTM	Universal Testing Machine
WEDM	Wire-Cut Electrical Discharge Machining
HSTR	High Strength and Temperature Resistive
EDM	Electrical Discharge Machining
FEM	Finite Element Method
CSV	Comma-Separated Values
BC	Boundary Condition
CAD	Computer Aided Design

CHAPTER 1

INTRODUCTION

1.1 RESEARCH BACKGROUND

Uniaxial fracture strain gathered from tensile test for plane specimen are not accurate because the result was calculated based on the average of entire critical cross-section of the specimen. Previous researches show that the fracture strain of plane specimens is not identical across the cross-section.

As reported by most of researchers, the failed plane specimen (after tensile test) shows a shape of saddle as shown in Figure 1.1. Final cross-section of plane specimen is totally changes against its original shape. Therefore, the equation to determine the stress and strain subjected to the specimen (force divided by area) is no longer accurate. In this study the true uniaxial ductile fracture strain of plane specimen will be investigated.

The study was focusing on three different materials which are carbon steel, aluminum and brass. The tensile test has been performed on all material studies to determine the engineering stress-strain curve. The curve obtained from the test then was converted to true engineering stress-strain curve. Then, true plastic stress-strain data was determined to be employed in Finite Element Analysis. In order to determine the uniaxial fracture strain, tensile test will be simulated in Finite Element software.

For this purpose, MSC Patran/Marc 2008r1 was applied. The engineering stress-strain curve from the Finite Element Analysis will be combined with experimental data in order to determine the fracture initiation point. The state of stress for each element in critical cross-section at fracture point then was investigated to determine the uniaxial fracture strain. Finally the result from the experiment has been compared with Finite Element results.

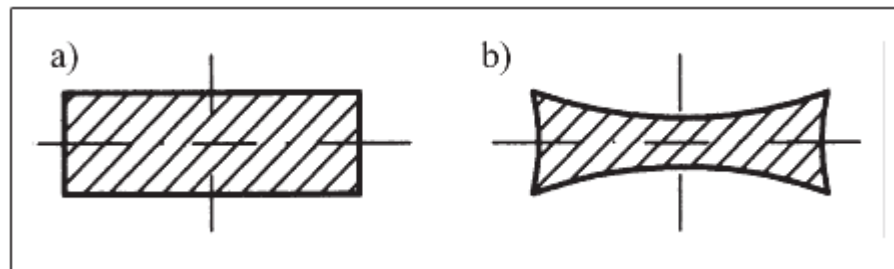


Figure 1.1: Cross-sectional area in the neck at fracture: a) before fracture, b) after fracture

Source: Kut, 2010

1.2 PROBLEM STATEMENT

Design is one of the important process in developing the engineering structure. During design stage, few processes were involved such as analysis of deflection, stress analysis, cost reliability and others. Stress analysis appears as a crucial process as many engineering structure fail due to lack of consideration on this analysis. One of the important parameters involve in stress analysis is uniaxial fracture strain. The failure on engineering structure normally predicted based on maximum stress or strain that can be withstand by the structure. Therefore, the fracture strain becomes crucial to be determined.

As discussed in previous section, the fracture strain can be determined by conducting the uniaxial tensile test. However, as reported by many researchers, the uniaxial fracture strain is very difficult to determined using plane specimens. It is due to the obvious changes in cross-section of plane specimen after tensile test was performed. Many researchers had tried to develop a simple method to calculate or determine the uniaxial fracture strain of the materials. However, there is no reliable method was reported recently.

1.3 OBJECTIVES

The objectives of the research are as follow:

- 1) To determine the uniaxial ductile fracture strain during tensile test of plane specimen
- 2) To investigate the state of stress of plane specimen during uniaxial tensile test.

1.4 SCOPES OF STUDY

The scopes of the research are as follow:

- 1) Specimen preparation
- 2) Materials used were carbon steel, brass and aluminum.
- 3) Plane specimen with rectangular cross-section
- 4) Uniaxial tensile test – at room temperature and refer to ASTM E8 2008
- 5) Finite Element Analysis (FEA)
 - MSC Patran/Marc
 - Non-linear
 - Large displacement
 - Homogeneous material and model
- 6) Validation – compare experiment data with finite element analysis result

CHAPTER 2

LITERATURE REVIEW

2.1 INTRODUCTION

This chapter will provide the detail description literature review done according to title of ductile fracture strain in uniaxial tensile test of plane specimen. Literature regarding any development or experiment about fracture strain and state of stress is useful in this project. This is includes the experiment setup, engineering and true stress-strain curve, and finite element analysis software available for analysis.

2.2 EXPERIMENTAL TEST SETUP

The uniaxial tension test is widely used to provide basic information on the mechanical behavior of materials and as an acceptance test for the specification of materials. In this test, a specimen is subjected to a continually increasing uniaxial tensile force while simultaneous observations are made of the extension of the specimen. Load–extension curves are used to construct stress–strain curves, which can provide more useful information on mechanical properties of materials. The most common properties derived from such curves are yield and ultimate strength values, elongation, and reduction of area (Mahmudi, Mohammadi and Sepehrband, 2004).

Flat specimens are machined from thermo mechanically rolled steel plate BV-DH32 with 36 mm thickness. This grade of steel is almost exclusively utilized in shipbuilding for the construction of structural parts of ships and offshore platforms. From mill sheets for the mother plate, the chemical compositions are shown in Table 2.1. Typical mechanical properties at room temperature are summarized in Table 2.2 where the values in parentheses are from mill sheets for the mother plate. As for parallel direction to rolling, three pairs of smooth flat specimens (P33, P34 and P35) are prepared so as to have different aspect ratios by changing thicknesses.

Actual dimensions at the reduced section are listed in Table 2.3. The experiments are conducted with a 300 kN UTM with controlled displacement. With a gauge length of 50 mm, a constant loading speed of 1 mm/min is applied. The loading is stopped every 1mm or 2 mm extension of gauge length to measure the actual thickness and breadth changes at the minimum cross section. Thickness and breadth are manually measured, with digital calipers and micrometer, at the six longitudinally different points to search the minimum cross section even before the onset of necking.

After the onset of necking, six points at the smallest cross section are measured for every increment due to the cushioning effect of specimens with rectangular cross section. Square grids are stenciled on the surface of the breadth side of the specimen to analyze digital images recorded during every test increment same as shown in Figure 2.1. Digital images are taken with a digital camera with a resolution of 2816×2112 pixels. The camera is mounted on a digital height gage to keep consistent barrelling distortion due to lens convexity during elongation of the specimen (Choung and Cho, 2008).

Table 2.1: Chemical composition of BV-DH32 steel

C	Si	Mn	P	S	Cu	Ni	Cr	Mo
0.14	0.28	1.06	0.012	0.003	0.03	0.02	0.03	0.01

Source: Choung and Cho, 2008

Table 2.2: Typical mechanical properties of BV-DH32 steel

Minimum yield strength	Minimum tensile strength	Minimum elongation
315 (355) MPa	440 (480) MPa	22(31) %

Source: Choung and Cho, 2008

Table 2.3: Breadth and thickness in reduced section

No.	b_0	t_0	b_0/t_0
P33	12.044	12.523	0.962
P34	12.030	9.000	1.337
P35	11.950	4.974	2.402

Source: Choung and Cho, 2008

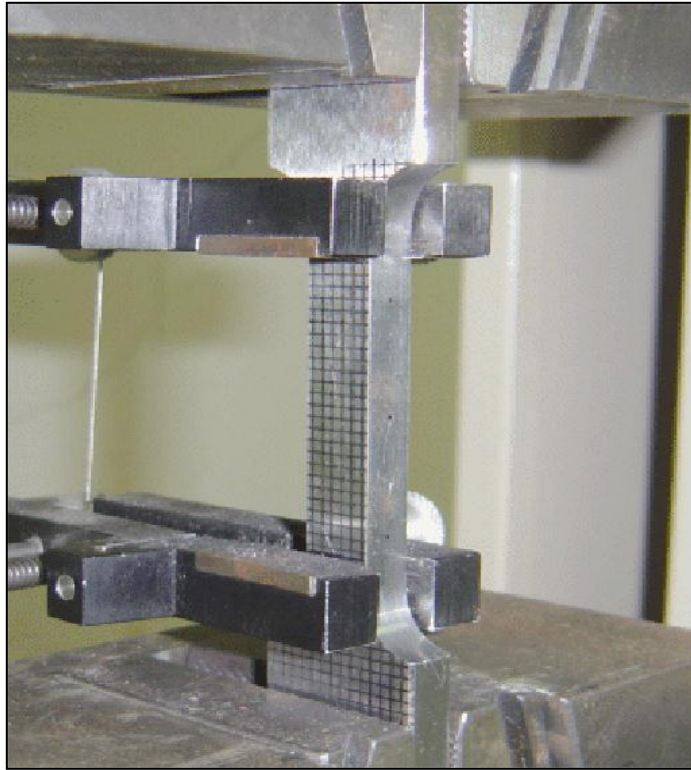


Figure 2.1: A photo of test set up for specimen P34

Source: Choung and Cho, 2008

2.3 WIRE-CUT EDM REVIEW

Wire-cut electrical discharge machining (WEDM) technology has grown tremendously since it was first applied more than 30 years ago. Its broad capabilities have allowed it to encompass the production, aerospace and automotive industries and virtually all areas of conductive material machining. This is because wire EDM provides the best alternative or sometimes the only alternative for machining conductive, exotic and high strength and temperature resistive (HSTR) materials with the scope of generating intricate shapes and profiles. It has proved to have tremendous potential in its applicability in the present day metal cutting industry for achieving a considerable dimensional accuracy, surface finish and contour generation features of products or parts.

WEDM is a thermo-electrical process in which material is eroded from the workpiece by a series of discrete sparks between the workpiece and the wire electrode (tool) separated by a thin film of dielectric fluid (deionised water) which is continuously forced fed to the machining zone to flush away the eroded particles. The movement of the wire is controlled numerically to achieve the desired three-dimensional shape and accuracy for the workpiece. Although, the average cutting speed, relative machining costs, accuracy and surface finish have been improved several times better since the commercial inception of the machine, further improvement is still required to meet the increasing demand of precision and accuracy by different industries.

However, so far precision and accuracy are concerned; the vibrational behaviour and the static deflection of the wire (wire lag) need to be studied simultaneously. Although a good number of researches have been carried out to study the wire lag and its measurement, a very little study has been done over the vibrational behavior of the wire due to numerous complexities.

The complexities arise out in modeling the wire-tool vibration phenomenon, in the solution approach of the vibration equation and also in conducting the experiments for the purpose of measuring the amplitude of the vibration. This originates the necessity to investigate into the vibrational behaviour of the wire in detail as the same plays a major role to decide the precision and accuracy of an electro-discharge machined job (Puri and Bhattacharyya, 2003).

2.4 ENGINEERING STRESS-STRAIN CURVE

The engineering tension test is widely used to provide basic design information on the strength of materials and as an acceptance test for the specification of materials. In the tension test a specimen is subjected to a continually increasing uniaxial tensile force while simultaneous observations are made of the elongation of the specimen.

The shape and magnitude of the stress-strain curve of a metal will depend on its composition, heat treatment, prior history of plastic deformation, and the strain rate, temperature, and state of stress imposed during the testing. The parameters, which are used to describe the stress-strain curve of a metal, are the tensile strength, yield strength or yield point, percent elongation, and reduction of area. The first two are strength parameters; the last two indicate ductility.

An example of the engineering stress-strain curve for a typical engineering alloy is shown in Figure 2.2. From it some very important properties can be determined. The elastic modulus, the yield strength, the ultimate tensile strength, and the fracture strain are all clearly exhibited in an accurately constructed stress strain curve.

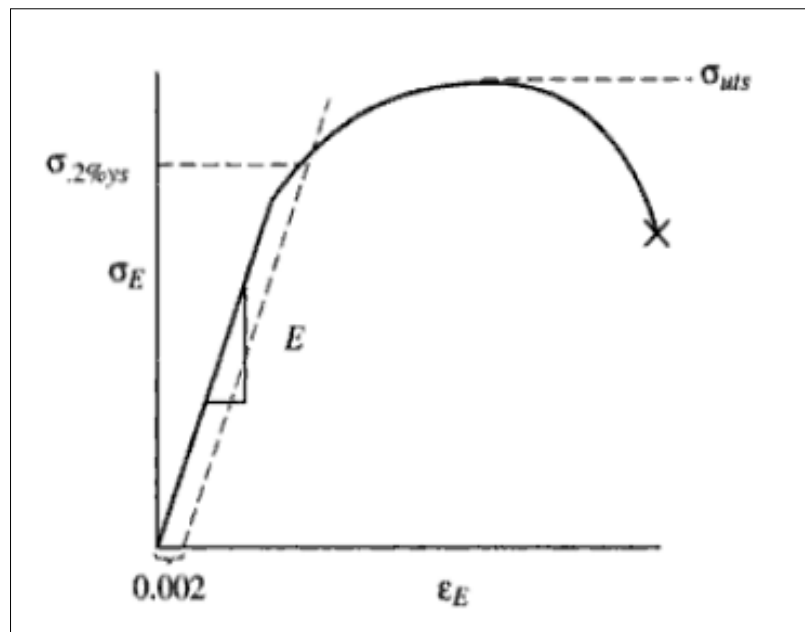


Figure 2.2: Engineering stress strain curve for a typical engineering alloy

The elastic modulus, E (Young's modulus) is the slope of the elastic portion of the curve (the steep, linear region) because E is the proportionality constant relating stress and strain during elastic deformation: $\sigma = E\varepsilon$. The 0.2% offset yield strength is the stress value, $\sigma_{0.2\%YS}$ of the intersection of a line (called the offset) constructed parallel to the elastic portion of the curve but offset to the right by a strain of 0.002. It represents the onset of plastic deformation.

The ultimate tensile strength is the engineering stress value or σ_{uts} , at the maximum of the engineering stress-strain curve. It represents the maximum load, for that original area, that the sample can sustain without undergoing the instability of necking, which will lead inexorably to fracture. The fracture strain is the engineering strain value at which fracture occurred.

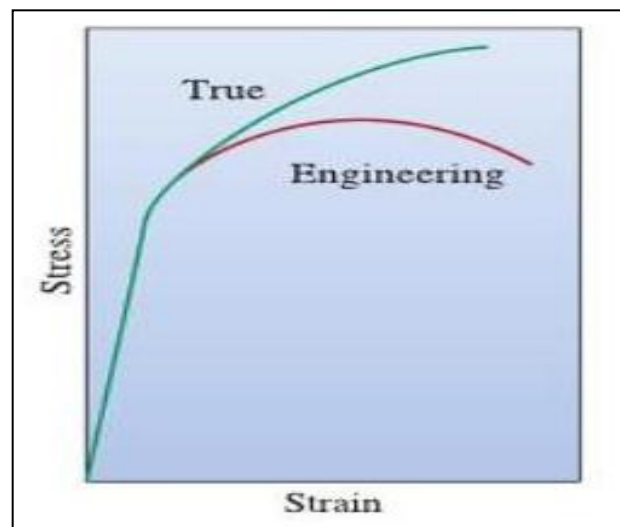


Figure 2.3: Comparison of engineering and true stress-strain curves

The engineering stress is the load borne by the sample divided by a constant, the original area. The true stress is the load borne by the sample divided by a variable the instantaneous area. Note that the true stress always rises in the plastic, whereas the engineering stress rises and then falls after going through a maximum.

The maximum represents a significant difference between the engineering stress-strain curve and the true stress-strain curve. Figure 2.3 show the comparison of engineering and true stress-strain curves. In the engineering stress-strain curve, this point indicates the beginning of necking. The ultimate tensile strength is the maximum load measured in the tension test divided by the original area. The engineering measures of stress and strain denoted in this module as σ_e and ε_e respectively, are determined from the measured the load and deflection using the original specimen cross-sectional area A_0 and length L_0 as equation (2.1) and (2.2):

$$\sigma_e = \frac{P}{A_0} \quad (2.1)$$

$$\varepsilon_e = \frac{\Delta L}{L_0} \quad (2.2)$$

2.5 TRUE STRESS-STRAIN CURVE

During stress testing of a material sample, the stress–strain curve is a graphical representation of the relationship between stress, obtained from measuring the load applied on the sample, and strain, derived from measuring the deformation of the sample. The nature of the curve varies from material to material.

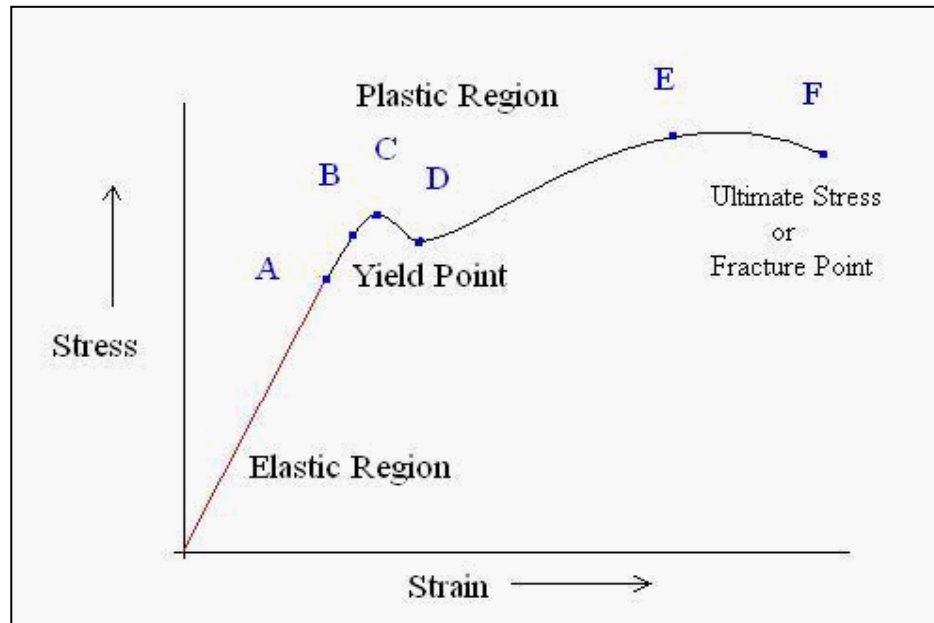


Figure 2.4: Typical stress-strain curve

- Point A: At origin, there is no initial stress or strain in the test piece. Up to point A Hooke's Law is obeyed according to which stress is directly proportional to strain. That's why the point A is also known as proportional limit. This straight line region is known as elastic region and the material can regain its original shape after removal of load.
- Point B: The portion of the curve between AB is not a straight line and strain increases faster than stress at all points on the curve beyond point A. Point B is the point after which any continuous stress results in permanent, or inelastic deformation. Thus, point B is known as the elastic limit or yield point.
- Point C & D: Beyond the point B, the material goes to the plastic stage till the point C is reached. At this point the cross-sectional area of the material starts decreasing and the stress decreases to point D. At point D the workpiece changes its length with a little or without any increase in stress up to point E.

- Point E: Point E indicates the location of the value of the ultimate stress. The portion DE is called the yielding of the material at constant stress. From point E onwards, the strength of the material increases and requires more stress for deformation, until point F is reached.
- Point F: A material is considered to have completely failed once it reaches the ultimate stress. The point of fracture, or the actual tearing of the material, does not occur until point F . The point F is also called ultimate point or fracture point.

Therefore, availability of a method similar in principle to (Zhang and Li, 1994) approach but much simpler is highly desirable. A power law is often used to represent the whole flow curve, for instance $\sigma = K\varepsilon^n$, where K and n are empirical constants determined from known true stress-strain data before necking Figure 2.5.

Modern FEA programs do not require input of the uniaxial true stress-strain function in analytical form. It is entered numerically as ordered pairs taken from experimental data and the power law or any other function in analytical form are not necessary for curve fitting the measured true stress-strain data before necking. The power law may be useful for extrapolation of the true stress-strain curve beyond necking (Ling, 1996).

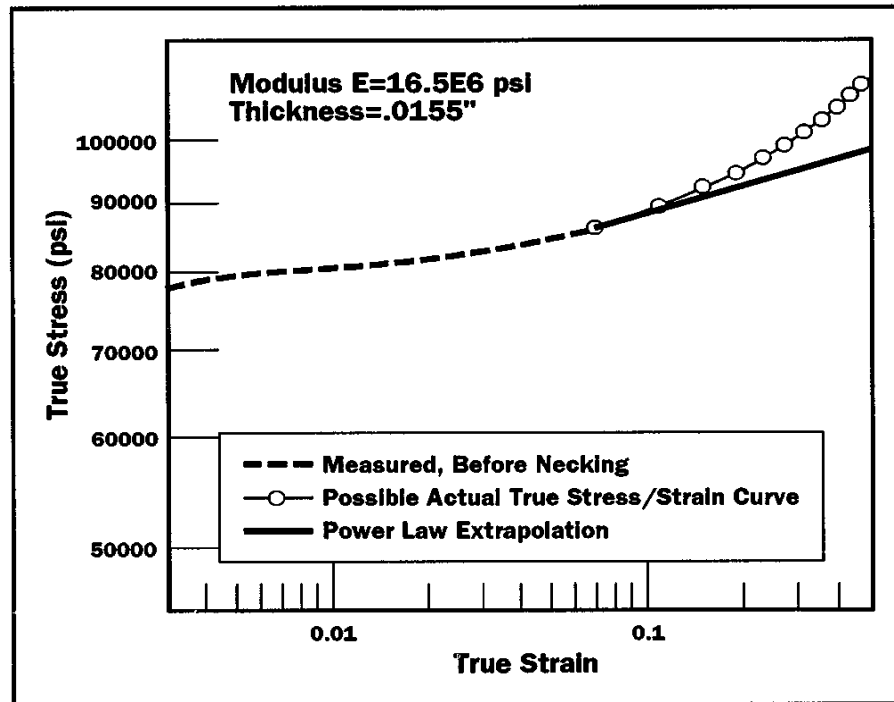


Figure 2.5: Example of true stress-strain plot

Source: Ling, 1996

True stress–strain curves can be obtained using tensile (Bridgman, 1952; Cabezas and Celentano, 2004; Koc and Stok, 2004; Komori, 2002; Mirone, 2004; Zhang, 1995; Zhang et al., 1999), compression, ball indentation, punch, torsion, and notch tensile tests. Haddadi et al. (2006) and Bouvier et al. (2006) studied the anisotropic behaviors of sheet metals under large plastic deformations using the simple shear test. Most of these methods obtain true stress–strain relations only for strains less than 0.5. However, the maximum strain often exceeds 1.0 in bulk metal forming, such as in forging, extrusion, and rolling. Sometimes it reaches 3.0 in multi-stage automatic cold forging, the so-called cold-former forging used to produce fasteners.

Recently, many researchers have tried to obtain true stress–strain curves using finite element methods, see e.g. (Cabezas and Celentano, 2004; Campitelli et al., 2004; Choi et al., 1997; Husain et al., 2004; Isselin et al., 2006; Lee et al., 2005; Mirone, 2004; Nayebi et al., 2002; Springmann and Kuna, 2005). In a tensile test, the true strain reaches its maximum value at the smallest cross-section in the necked region, and it may exceed 1.5 just before a ductile material fractures. Therefore, one should be able to obtain the flow stress of materials at a large strain if finite element methods are used to predict the localized deformation behavior during a tensile test. A few researchers have attempted to obtain the flow stress at a large strain using simulation and experimental approaches, but these applications have been quite limited, see e.g. (Cabezas and Celentano, 2004; Mirone, 2004).

2.6 FINITE ELEMENT ANALYSIS (FEA) SIMULATION

Numerical simulation of steel tensile specimen has been performed using MSC Marc Mentat software, which enables solving non-linear and contact problems. FEM simulation's geometrical model has been created based on the experimental model. The purpose of the numerical simulation in this case is neither detailed analysis of stresses and strains nor determining their values. The purpose of the simulation is to indicate the area, where the state of stress on the tensioned specimen is the closest to uniaxial tension, within an entire strain range up to specimen tensile failure. Therefore the specimen tension process has been analyzed in the plane stress condition.

The tension simulation has been performed until specimen tensile failure, and it corresponds to extensometer (II) displacement, which was 15.33 mm for the steel specimen. The tensile force curves have been prepared and compared in order to validate the FEM simulation. The limit value of ductile fracture strain depends on the present state of stress.

In the mechanical & mathematical modeling approach, non-dimensional stress triaxiality, $k = \sigma_m / \sigma_H$, where σ_m is a mean normal stress, σ_H is an equivalent stress, is the very important parameter, which unequivocally specifies the plane state of stress that shown in Figure 2.6. If this factor is known, it is possible to determine the state of stress in any point of strained object, e.g.: if $k = 0$ – this is a simple shear that shown in Figure 2.6.c), $k = 0.66$ – it is a biaxial regular tension that shown in Figure 2.6.e), $k = -0.33$ – it is an uniaxial compression that shown in Figure 2.6.b), and etc.

In considered case we determine the strain for the tensile test, so that k factor value is 0.33. As seen in FEM calculations, the uniaxial state of stress is present in an initial tension phase and lasts until the neck is created, and then once R_m limit is exceeded, the states of stress in individual zones differ significantly same as shown in Figure 2.7.

The state of stress in the lateral zone L changes slightly in the biaxial tension direction, reaching $k = 0.36$ in its final phase. Whereas the state of stress in the middle zone S changes significantly in the simple shear direction, reaching $k = 0.106$ in its final phase (Kut, 2010).

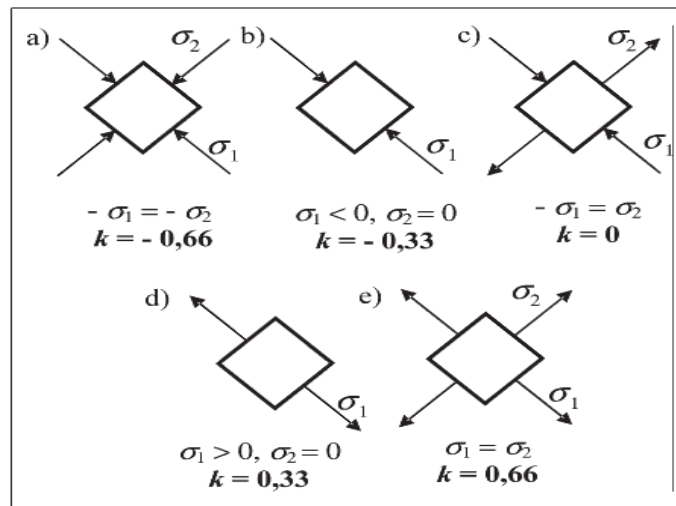


Figure 2.6: Stress triaxiality, k for an individual plane stress cases:
 a) biaxial compression, b) uniaxial compression, c) simple shear
 d) uniaxial tension e) biaxial tension

Source: Kut, 2010

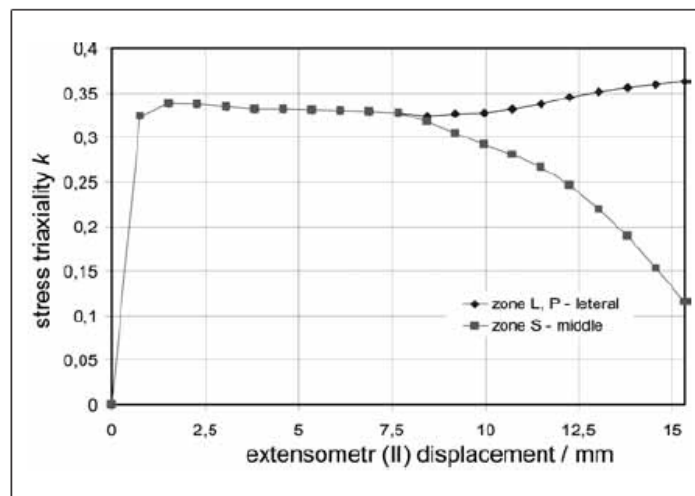


Figure 2.7: Comparison of stress triaxiality in different specimen zone:
L, P – lateral, *S* – middle

Source: Kut, 2010

When the aspect ratio is 1.0, thickness and breadth reduction rates are the same regardless of hardening exponents. However, the bigger the aspect ratio or the smaller the plastic hardening exponent, the larger the thickness reduction than the breadth reduction. Therefore, for specimens with large aspect ratios and small plastic hardening exponents, early fracture is subject to occur.

Zhang et al (1999) perceived differences between two area reduction rates and considered thickness reduction rates to be a proportional reduction, of which concept is analogous to diametric reduction of a round specimen. In the authors' opinion, recovered thickness at the center of breadth direction does not completely represent thickness reduction because of cushioning effect as shown in Figure 2.8. Scheider et al (2004) assumed that even after onset of necking, $t_0 / t = b_0 / b$ is effective. But this assumption is proved to be invalid during non-uniform deformation except when initial thickness and breadth are identical (Choung and Cho, 2008).

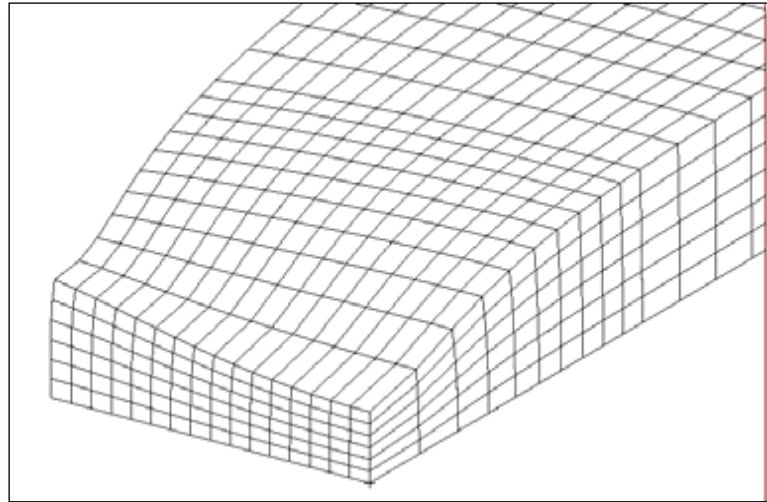


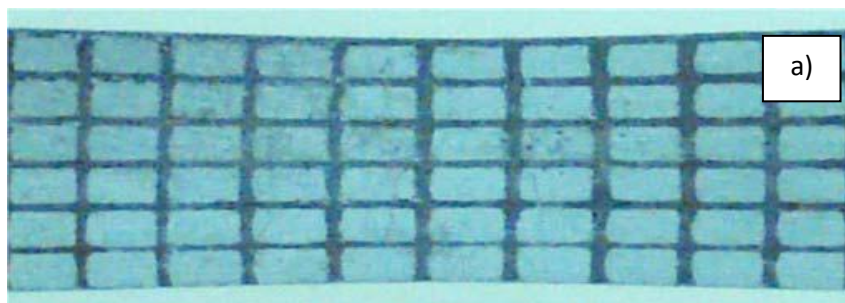
Figure 2.8: Shape of plane specimen at fracture point obtained from Finite Element Analysis (FEA)

Source: Choung and Cho, 2008

2.7 STRESS TRIAXIALITY AND DUCTILE FRACTURE STRAIN

The ultimate ductile fracture strain determination method for the specimen of circular cross-section has been presented by FEM method. The state of stress in individual locations of tensile tested specimen in successive process phases has been determined unequivocally with the stress triaxiality k . It has been demonstrated that the plane specimen's fracture strain value in the fracture location varies and depends on the state of stress, which is present in the final specimen's tension phase. The ductile fracture strain values in various fracture locations for steel, brass and aluminum specimen have been experimentally determined and compared. The simple and practical method to determine this strain has been proposed (Kut, 2010).

Then, the cushioning effect is most obvious for P33, which is close to unit aspect ratio, the deviation between manual measurement and photo analysis is increased for the specimens with the larger aspect ratio. The moving grids at $\varepsilon_p = 0.41$ and $\varepsilon_p = 1.42$ (just previous step of fracture) for P33 are represented in Figure 2.9. The mechanical properties obtained from experiments are shown in Table 2.4 where the hardening exponent n and strength coefficient K are derived by using Hollomon's power law. On the other hand, true fracture strain is determined from measurements of actual area reductions (Choung and Cho, 2008).



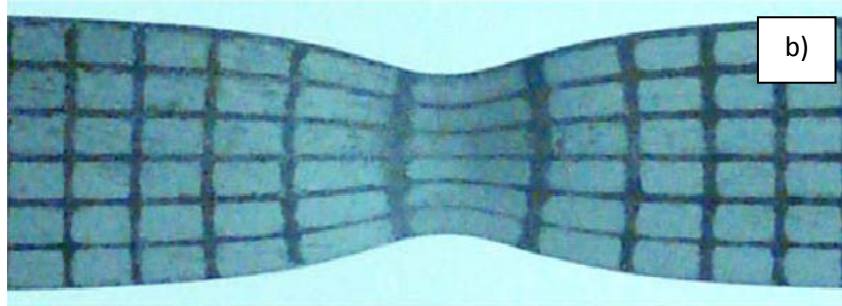


Figure 2.9: The moving grids in local necking zone: a) $\varepsilon_p = 0.41$, and
b) $\varepsilon_p = 1.42$ (close to fracture)

Source: Choung and Cho, 2008

Table 2.4: Mechanical properties of BV Grade DH32 steel

	σ_y (MPa)	σ_u (MPa)	n	K (MPa)	ε_f
P33	360.2	493.7	0.283	968.7	1.55
P34	358.0	494.0	0.263	938.9	1.50
P35	364.9	512.1	0.273	981.6	1.72

Source: Choung and Cho, 2008

Previous research of ICL shows that the crack initiates at the center of the dog-bone specimen in a tensile test. Therefore, the equivalent plastic strains of the central element at the fracture elongation point obtained from the numerical models were summarized in Table 2.5 and compared with the fracture strain measure from thickness and width reduction of specimens (low precision). Again, model 3 gives the best prediction of the local equivalent strain to fracture.

Hence, one can conclude that the model with solid elements and isotropic plasticity model can give accurate numerical prediction for the dog-bone specimen tensile tests. The reason why the shell element cannot give good prediction might be that the width thickness ratio of the specimen cross-section is not big enough for a shell assumption.

One can also obtain the stress triaxiality information (negative pressure divided by effective stress) of the central point of the specimen from numerical simulation. The evolution of stress triaxiality with the elongation of the gauge section is shown in Figure 2.10. The average triaxiality value up to fracture is about 0.345, and the triaxiality before necking is exactly equal to the analytical value $1/3$. The average stress triaxiality would be used for fracture calibration together with the fracture strain (Meng Luo, 2008).

Table 2.5: Comparison of equivalent strain to fracture of dog-bone specimen between simulations and test of dog-bone specimens

	Model 1	Model 2	Model 3	Model 4	Measurement after test
Fracture strain	0.12	0.13	0.48	0.10	0.53

Source: Meng Luo, 2008

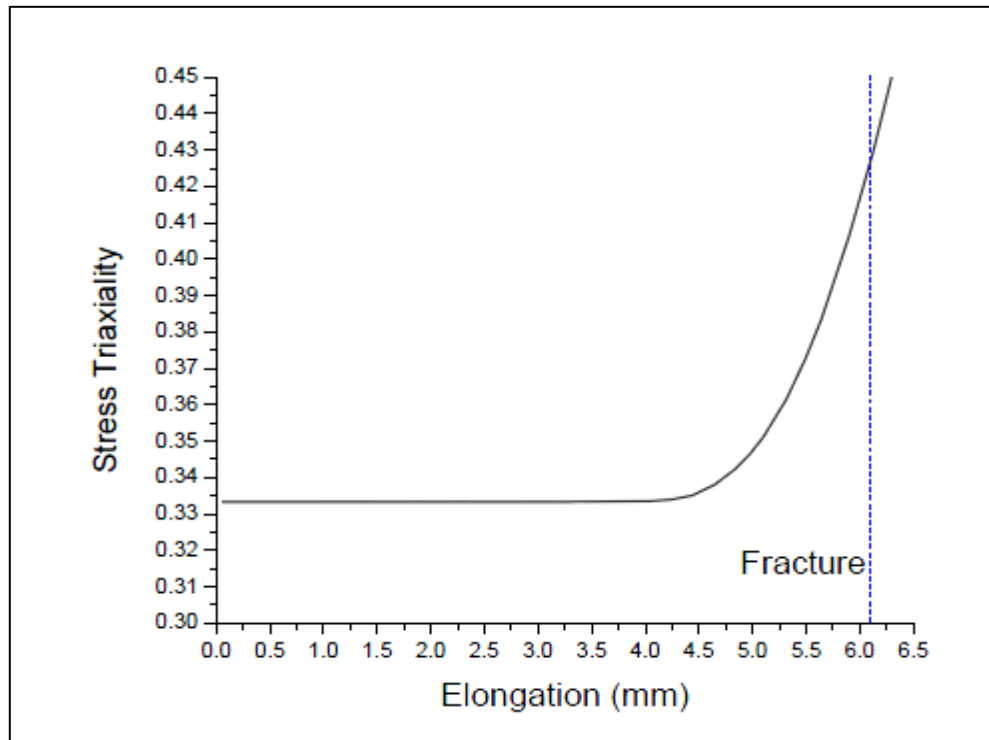


Figure 2.10: The evolution of stress triaxiality calculated by ADINA software

Source: Meng Luo, 2008

CHAPTER 3

METHODOLOGY

3.1 INTRODUCTION

In this chapter, all process involve from the beginning of the project until end has been stated. It is to make sure all suitable and affordable process occurred during the project and make it easily to refer. Then, the process flow chart can be easy the work to do because it will show step by step the process in this project. So, the arrangement of this report will become more structure and easily to understand.

In order to finish this project smooth and clearly, the method used must be clear. Methodology also include all about process from starting until end of this project. This chapter will cover about specimen preparation, wire cut process, polishing specimen, tensile test, finite element analysis (FEA) and etc.

3.2 RESEARCH FLOW CHART

The process flow chart represents in Figure 3.1 was showing the arrangement of flow chart in order to finish this project. It was started with introduction and then literature review, specimen preparation and tensile test processes. This step must be done step by step. After that are analysis of the result and finite element analysis. In the finite element analysis there is results that need to decide whether to accept or reject. Lastly is report writing process in order to conclude this project clearly.

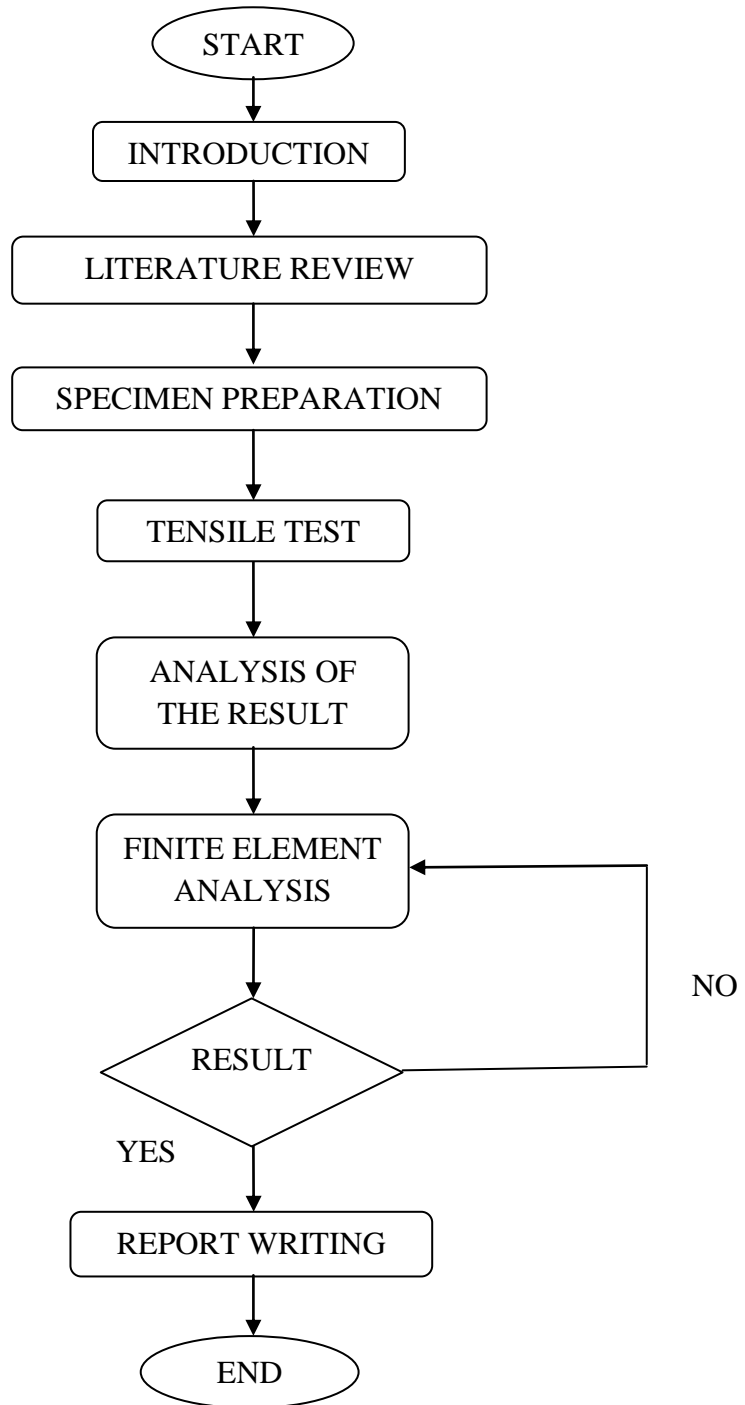


Figure 3.1: Research flow chart

3.3 SPECIMEN PREPARATION

3.3.1 Specimen Specification

For tensile test, three type of materials have been prepared. Three specimens have been machined for each material. The materials used are aluminum, brass and mild steel. In order to reduce the experimental error, three specimens for each material have been prepared.

The specimen was machined according to ASTM E8 2008 specification for plane tensile test specimen. Based on ASTM E8 2008 that shows in Figure 3.2, the length of specimens that need to use in tensile test is 200 mm and thickness of 6 mm. However, the raw materials that available in store are in rod shape with diameter of 32 mm. The length needed for every material is 250 mm. In order to shape the specimen into tensile test specimen shape with rectangular cross-section, wire cut process has been done to cut the raw material. The wire cut machine has a cutting range limit and clamping area is needed in order to clamp the materials. About 40 mm from the material has been used to clamp the material until it cannot be moved. This process has been done to avoid the cutting process from any interference.

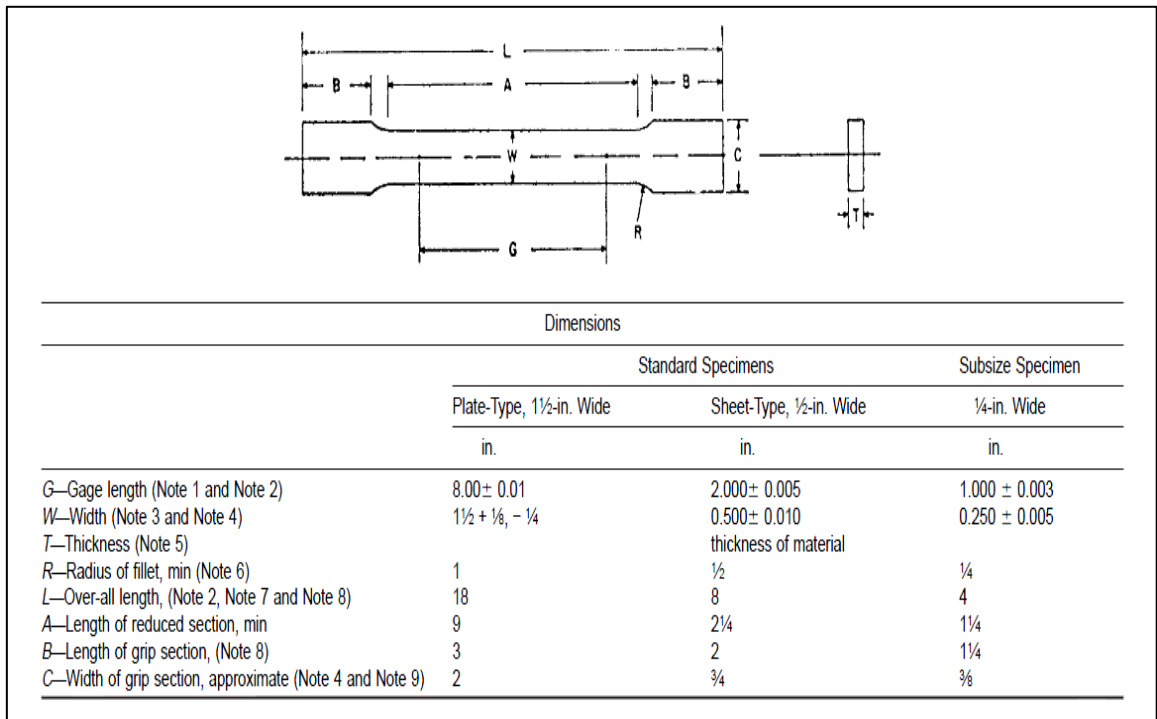


Figure 3.2: The standard ASTM tensile test dimension for plane specimen.

Source: ASTM E8, 2008

3.3.2 Machining Process

After finish the raw material cutting process for all material needed with diameter 32 mm and length 250 mm, the machining process was complicated process in this specimen preparation process. The process is to design the raw material become a tensile test specimen shape. First process is drawing the cutting line in the wire cut machine system. The Sodick machine has Sodick Linear Servo Controller software that can operate all the system in this Sodick machine. The software can read the drawing and then the wire has been used to cut the material by the shape that drawn in the system.

This machine uses a wire as the cutter to cut the material. Wire cut machine is very useful machine because it usually can solve many problem related with material

preparation. It can cut a difficult part or shape and also difficult angle. The wire use for this wire cut process is made from brass with diameter 0.25 mm that shown in Figure 3.3. An electric current will be used to operate this machine and also the electricity use to cut the material. The electric current will flow through the brass wire. This process is call Electric discharge machining (EDM).



Figure 3.3: The wire use to cut the material in wire cut machine.

Electric discharge machining (EDM), sometimes colloquially also referred to as spark machining, spark eroding, burning, die sinking or wire erosion, is a manufacturing process whereby a desired shape is obtained using electrical discharges (sparks). Material is removed from the workpiece by a series of rapidly recurring current discharges between two electrodes, separated by a dielectric liquid that shown in Figure 3.4 a) and subject to an electric voltage. The wire used is rotating that shown in Figure 3.4 b) to cut the material. After the wire through the material, the wire has not been used anymore and it has been disposed.

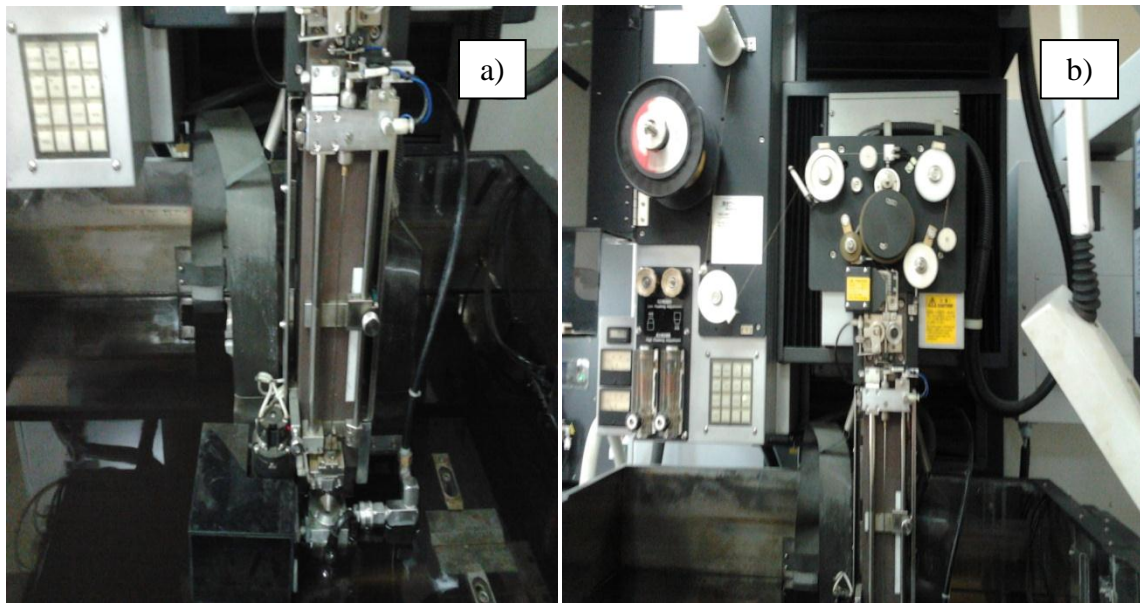


Figure 3.4: Wire cut machine: a) water is use as dielectric liquid, and b) wire rotating area

The software used in wire cut machine is Linear Servo Controller that is shown in Figure 3.5. After that, create the drawing by draw one straight line for first drawing same as shown in Figure 3.6. Then, for second drawing must be draw line and curve to get the tensile test specimen shape. Draw one side line and then mirror the line to get another side line same as shown in Figure 3.7. Next, the drawing was saved in this machine system.

The starting and ending point has been stated at the drawing line before start the cutting process to tell this system where to start and end the machining process. Don't forget to clamp the material at clamping area inside the tank. There are several holes with screw thread. These screw threads were used in clamping process to clamp the specimen and avoid any movement during machining process that can affect the specimen. Then, set the origin of X, Y and Z axis for a starting point that machine want to know before it start from the starting point at drawing in the software.

After finish all the process of setting machine, then it can be start the cutting process. The machine shield will close automatically and also water will be fulfilling the machine to cover and sink the entire specimen with water.

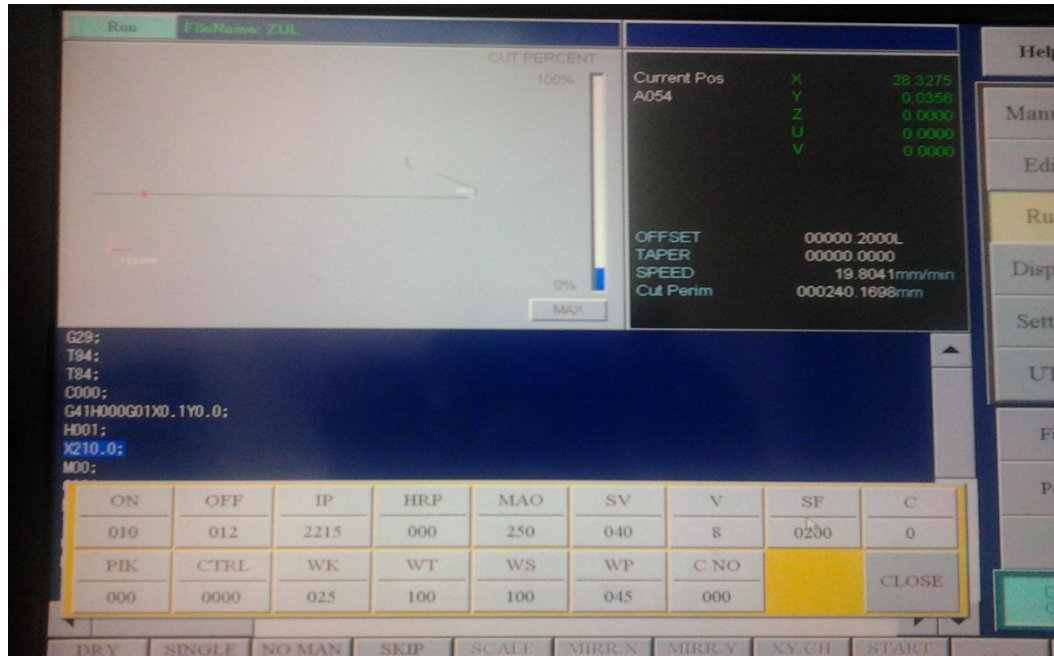


Figure 3.5: The software used to generate wire cut machine

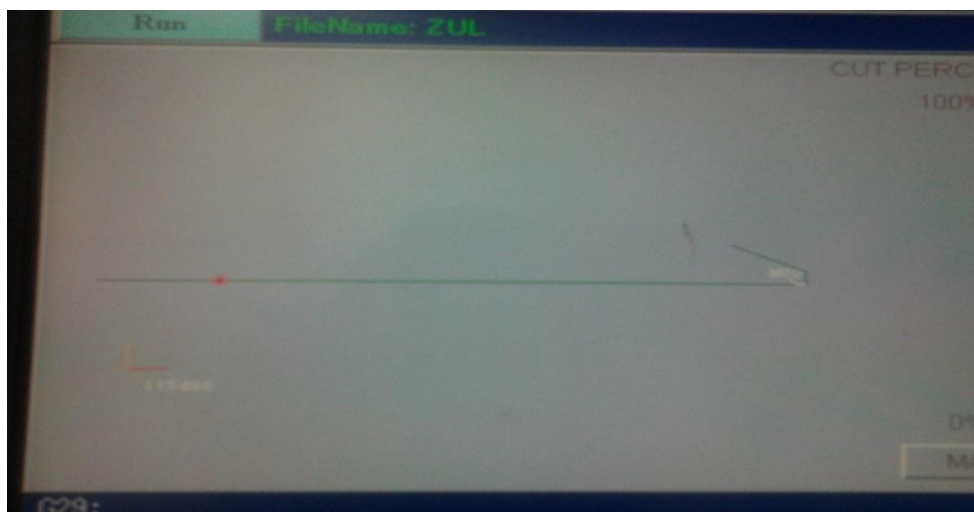


Figure 3.6: The straight line from wire cut drawing for first step of cutting the specimen.

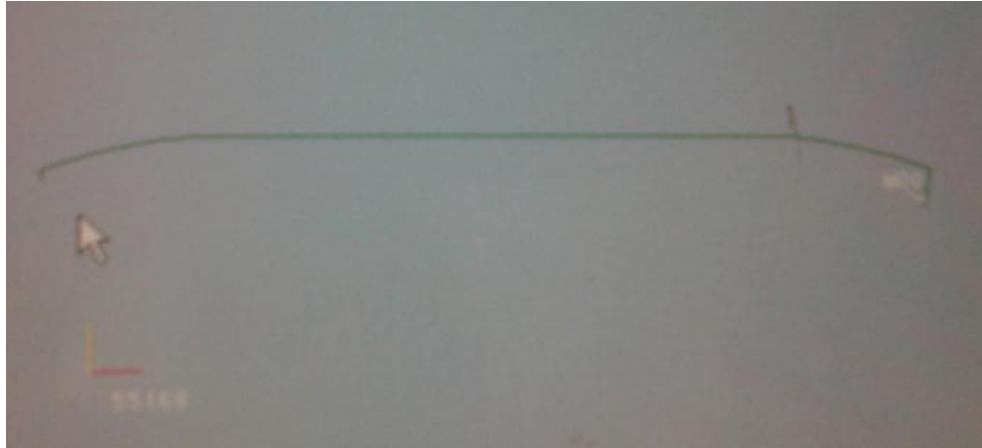


Figure 3.7: The second step of drawing that use in cutting material

3.3.3 Polishing Process

This process is quite messy work because need to clean the entire specimen surface until it become smooth and shiny. Sandpaper with difference grit number is use in this process. To obtain a good surface finish for the tensile test specimens, this process must be done slowly. Firstly use the small sandpaper grit number because it usually has rough surface to easily remove more unsuitable surface like scratch. Table 3.1 show the direction of polishing process for difference number of sandpaper grit.

Table 3.1: The direction of polishing process for difference sandpaper grit number

Sandpaper grit number	Polishing direction
100	Above and below
220	Right and left
600	Above and below
1000	Right and left
1200	Above and below
2000	Right and left

The best solution to obtain best surface finish is to do the polishing work under water flow. The specimen has become smooth and shiny just like a mirror same as shown in Figure 3.8. This is because water can remove all the dirty and waste from the sandpaper. It also makes the movement of sandpaper smooth and clear during the polishing process.



Figure 3.8: The surface finish after polishing using sandpaper

3.3.4 Zone Marking Process

The measuring bases to indicate the measuring zone have been marked on the specimen surface. *L*, *P* – Lateral, *S* – Middle. The zone width and specimen thickness have been measured in these locations before and after the specimen tensile failure. The geometrical values have been measured using the microscope with an accuracy of 0.01 mm.

The gauge length area (50mm) was highlighted with black marker same as shown in Figure 3.9 and the line marking was made same as Figure 3.10 in order to obtain the easiest way to see the marking zones under the optical microscope. Then the lines for *L*, *P* and *S* zones are marking by using scriber as shown in Figure 3.11 with just slow touch to obtain the straight lines. Hard marking can change the microstructure of the specimen and will be affect the result. Figure 3.12 show the example of marking zone at tensile test specimen from previous researcher.



Figure 3.9: The highlight region at gauge length

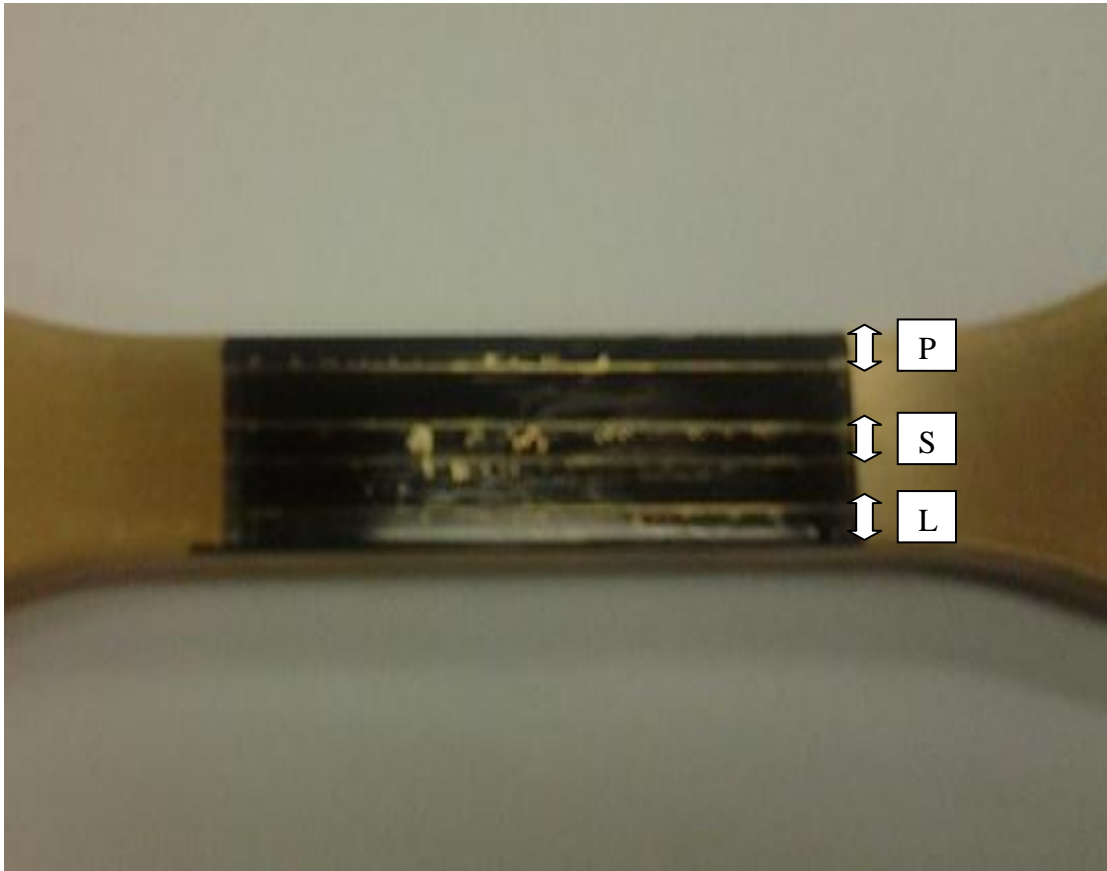


Figure 3.10: The marking zone with three zone: a) lateral-zone L and P, b) middle-zone S



Figure 3.11: The marking zone for aluminum specimen

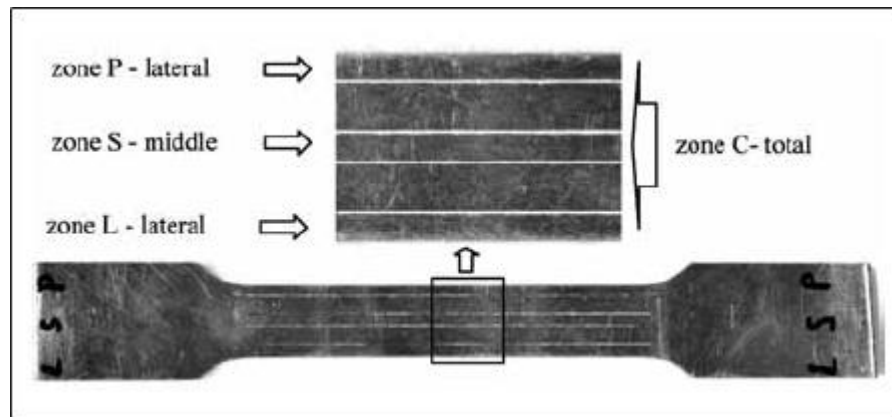


Figure 3.12: Example of marking zone at tensile specimen

Source: Kut, 2010

3.4 TENSILE TEST

One of the simplest tests for determining mechanical properties of a material is the tensile test. In this test, a load is applied along the longitudinal axis of a rectangular cross-section test specimen Figure 3.16. The applied load and the resulting elongation of the member are measured. In many cases, the process is repeated with increased load until the desired load levels are reached or the specimen breaks. Load-deformation data obtained from tensile tests do not give a direct indication of the material behavior, because they depend on the specimen geometry. In this project, the geometry of the specimen is plane specimen with rectangular cross-section area.

This tensile test experiment has been done by using SHIMADZU machine with maximum load is 100 kN. This machine can be used until maximum force or load about 90 kN. The strain rate or speed that use for this uniaxial tensile experiment is 0.5 mm. After that, the result of uniaxial tensile test form aluminum is show in Figure 3.13. From this result, the specimen elongate and break in the highlight area that is gauge length area. Same result occur at two others specimen those shows in Figure 3.14 and Figure 3.15 for brass and mild steel.



Figure 3.13: The specimen condition after break for aluminum



Figure 3.14: The specimen condition after break for brass



Figure 3.15: The specimen condition after break for mild steel



Figure 3.16: The specimen break during tensile test

3.5 MEASUREMENT OF ZONE LENGTH

After made marking at the gauge length in the specimen surface, the length of zone L , P and S was measured to confirm the actual length under optical microscope. By using dial gauge, the measurement was read before and after the tensile test experiment. The dial gauge sensor has been set to touch the microscope table and set it to zero. The zones were measured using microscope and move the table from start until end of the line for every zone. The length of the zone by read from dial gauge after measurement of every zone.

This measurement process has been done before and after the specimen break. It is because the data are used in calculation to get the ductile fracture strain at every zone. All the data are put in Table 4.6 in Chapter 4.

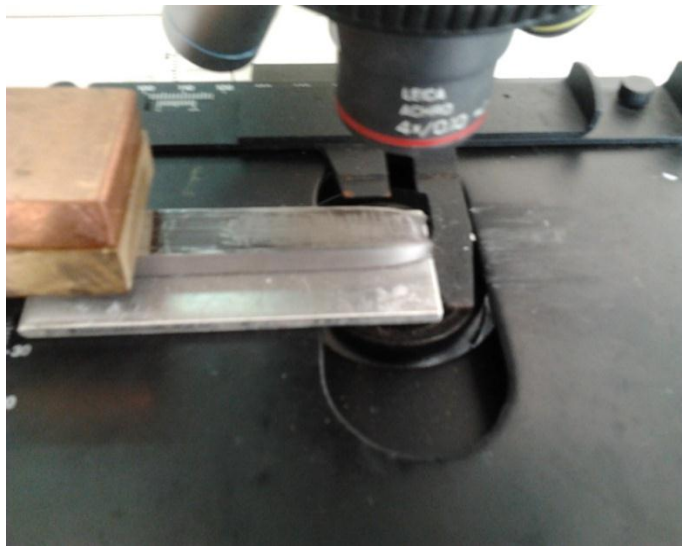


Figure 3.17: The position of specimen when using microscope



Figure 3.18: The position of dial gauge when during measurement



Figure 3.19: The measurement process by using microscope and dial gauge

3.6 FINITE ELEMENT ANALYSIS (FEA)

Last step is to put all data in Finite Element Analysis (FEA) to get the actual graph and result for the best ductile fracture strain and also stress triaxiality for uniaxial tension that needed is 0.33. This project is using Finite Element Analysis software name MSC PATRAN for pre-processing and post-processing. Besides that, MSC MARC is use as a solver in this project.

PATRAN is the world's most widely used pre/post-processing software for Finite Element Analysis (FEA), providing solid modeling, meshing, and analysis setup for MSC NASTRAN, Marc, ABAQUS, LS-DYNA, ANSYS, and Pam-Crash.

PATRAN provides a rich set of tools that streamline the creation of analysis ready models for linear, nonlinear, explicit dynamics, thermal, and other finite element solvers. From geometry cleanup tools that make it easy for engineers to deal with gaps and slivers in CAD, to solid modeling tools that enable creation of models from scratch, PATRAN makes it easy for anyone to create FE models. Meshes are easily created on surfaces and solids alike using fully automated meshing routines (including hex meshing), manual methods that provide more control, or combinations of both.

Finally, loads, boundary conditions, and analysis setup for most popular FE solvers is built in, minimizing the need to edit input decks. PATRAN's comprehensive and industry tested capabilities ensure that the virtual prototyping efforts provide results fast so that can be evaluated product performance against requirements and optimize the designs.

Figure 3.20.a) and Figure 3.20.b) are represented the distribution of stress triaxiality, k for initial and final phase of tensile test. In order to see the suitable result for this project, this distribution must be obtained to know the movement of stress triaxiality, k wheather near to biaxial tension for $k=0.66$, uniaxial tension $k=0.33$ or near to simple shear where $k=0$.

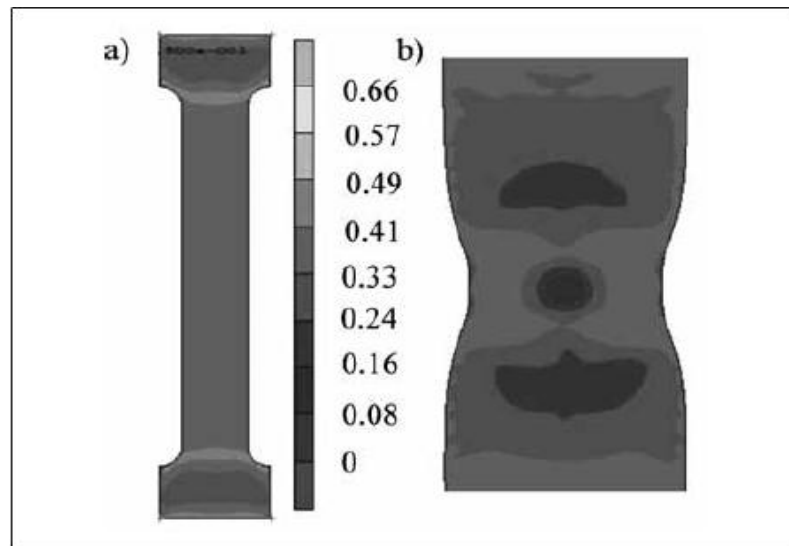


Figure 3.20: Distribution of stress triaxiality k :

a) Initial phase of tensile test, and b) Final phase of tensile test

Source: Kut, 2010

3.6.1 Modeling, Meshing and Solving Process

Modeling design was prepared by using Finite Element Analysis software that is MSC software PATRAN. In order to keep the calculation time as low as possible and in other hand obtain an accurate result. Firstly, one new folder was made for this project. All the data and result that has been done by using Finite Element Analysis was obtained in this folder.

Before that, the engineering stress-strain data was converted into true plastic stress-strain data in order to run the finite element analysis in MSC Patran/Marc 2008r1 software. Then, the data was saved in excel with CSV (comma delimited) format. Then, Patran 2008r1 software was opened and a new file was created to start the modeling process.

After that, setting the preferences and the analysis code was changed to MSC Marc. Then the modeling process has been started. Firstly, the GEOMETRY bar that shown in Figure 3.21 was taken to draw the specimen.

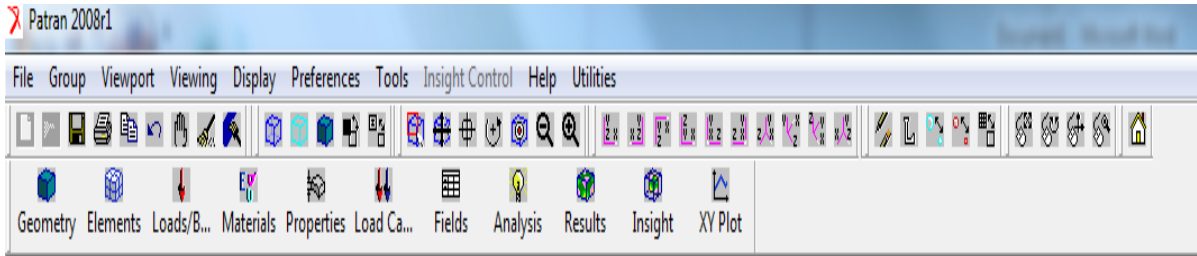


Figure 3.21: Step in PATRAN software

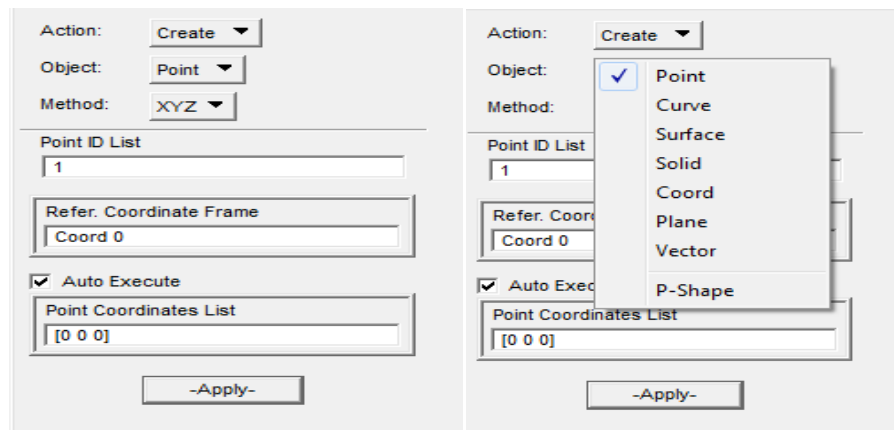


Figure 3.22: The setting for create a point coordinate

The specimen has been drawn in 2D (two dimension) by using coordinate to obtain the shape of specimen in quarter. Points are used to create the drawing part that is stated in Figure 3.22. In order to create the point, all point coordinate need to know. Figure 3.23.a) show the coordinate point for this project, while curve are used to create a line that combines two points together that is stated in Figure 3.23.b).

Then, surface was taken to create the surface for this shapes same as shown in Figure 3.23.c). However in this surface process, don't forget to change the direction of surface to become positive direction that already shown in Figure 3.23.d). Lastly create the solid to get the 3D (three dimension) specimen. The surface was extruded with the thickness needed (3 mm) that shown in Figure 3.24.

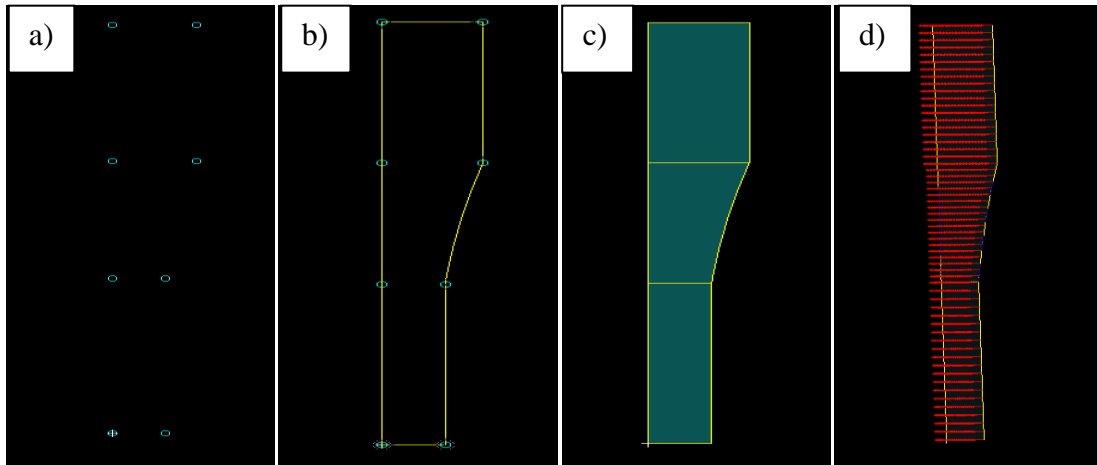


Figure 3.23: The step in GEOMETRY part from: a) point coordinate, b) make line to combine the point, c) make surface, and d) change surface direction.

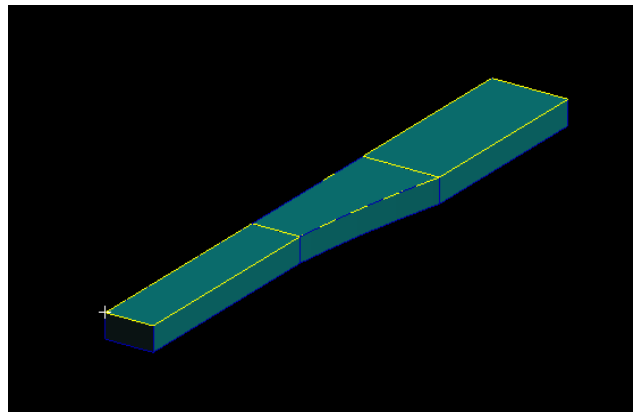


Figure 3.24: The solid part of the specimen in quarter shape

After that, the ELEMENT part for the specimen was created by using mesh. Figure 3.25.a) show the first step in ELEMENT part that is the mesh seed process for the specimen. In this project, two mesh seed are used to get the suitable meshes that are uniform and one way bias.

Figure 3.25.b) is showing the meshing process for the specimen used in this project. The mesh in solid type and element shape of hexagon are applied. After that, all the meshing has been equivalence to connect the mesh in the solid part of the specimen. The process is shown in Figure 3.25.c).

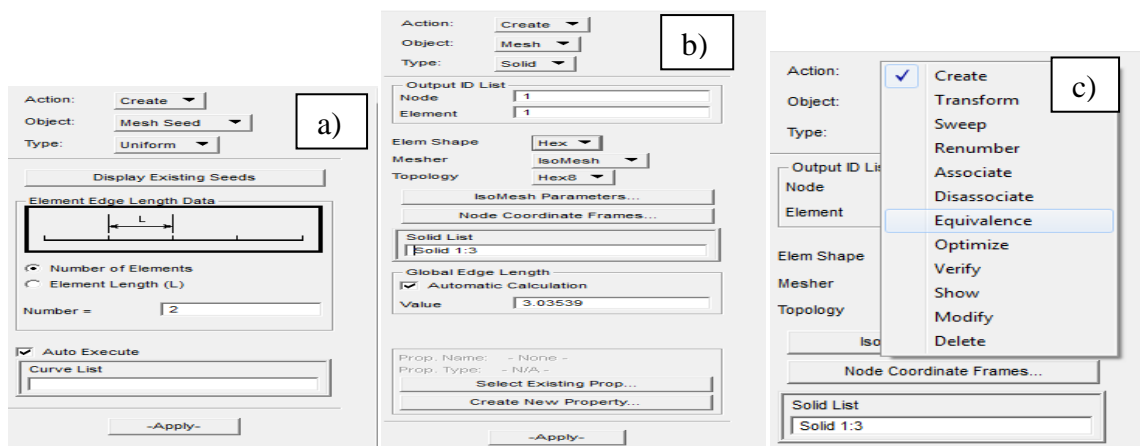


Figure 3.25: Step for ELEMENT part: a) mesh seed process, b) the meshing process and c) equivalence process

Then, LOADS/BCs (boundary condition) part must be applied to get the boundary condition at the specimen. Set new name for every load that needed. Then click input data and put the data for the load. There are two type of boundary condition need to apply at the specimen. First is the displacement (15mm) boundary condition that is representing as uniaxial tensile test in Y-direction upward. After that, apply boundary condition to represent as symmetry in X, Y and Z axis. Change the translations and rotations area to give the boundary conditions that shown in Figure 3.26. This symmetry must be apply to make sure the software read there are symmetry shape at others site of the axis. Next, the

application region for all the loads is applied. Lastly, the solid region is selected as an application region.

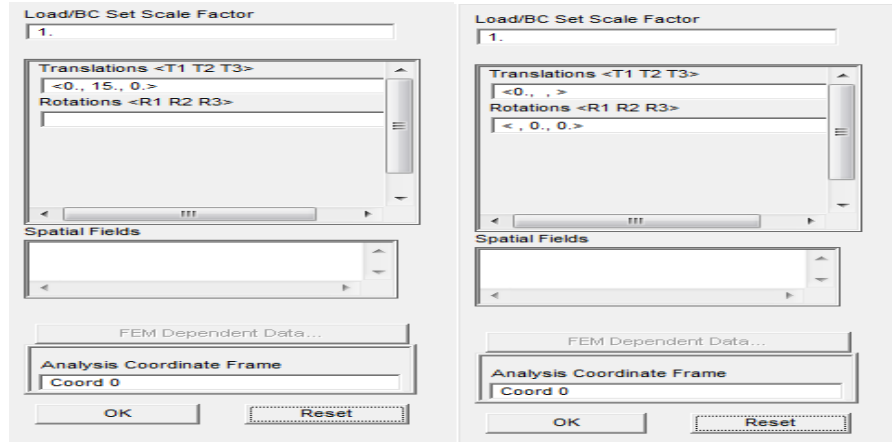


Figure 3.26: Step to create boundary condition at the specimen

Next, the FIELD part must be done to get the data before run this simulation. In this part, put all true plastic stress-strain data that save in early process. Change the object and method to material property and tabular input. Then, put any field name, click strain and input data to export the CSV file same as shown in Figure 3.27.

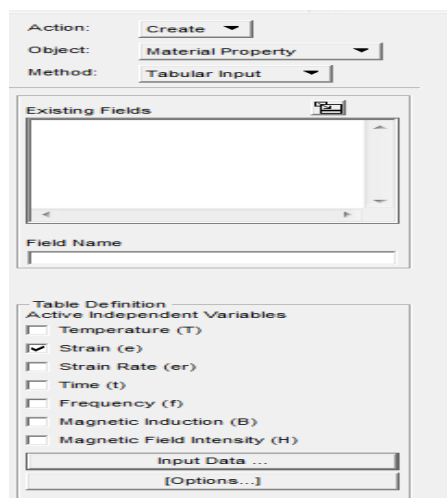


Figure 3.27: The FIELD part input data

The next step is to take the MATERIAL part and name the material. Click input properties to put all the data for elastic and plastic region. There are two importance data must be obtained in this part. Firstly is elastic region data that need to fill are young modulus and poison ratio of each material used. The value of young modulus and poison ratio for each material are stated in Table 3.2. Secondly is plastic region data that need to take from the FIELD part is true plastic stress-strain data for the material need to run.

Table 3.2: The value of young modulus and poison ratio for each material used

Material	Young Modulus (GPa)	Poison Ratio
Aluminum	70	0.33
Brass	100	0.34
Mild Steel	200	0.30

After that, the PROPERTIES part has been done to ensure the finite element analysis Patran 2008r1 software can read the properties given and run the simulation successful. The object part was changed to become 3D (3 dimension) in order to ensure the software read the specimen in 3D. Then, the properties name has given for this property.

After that, click option and take reduce integration for this part same as shown in Figure 3.28. For input properties, the box that shown in Figure 3.29 should be clicked and then took the data needed. Lastly, select the application region that needs to apply all the properties selected. This process is shown in Figure 3.30.

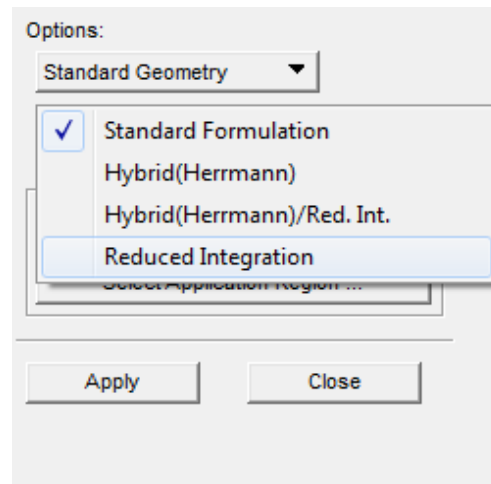


Figure 3.28: The PROPERTIES part to change the option into reduced integration

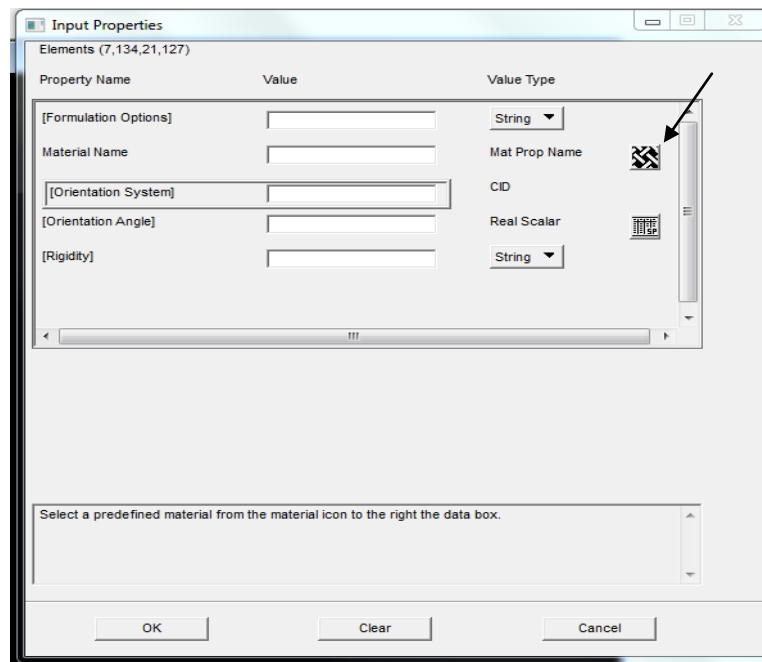


Figure 3.29: Input properties part.

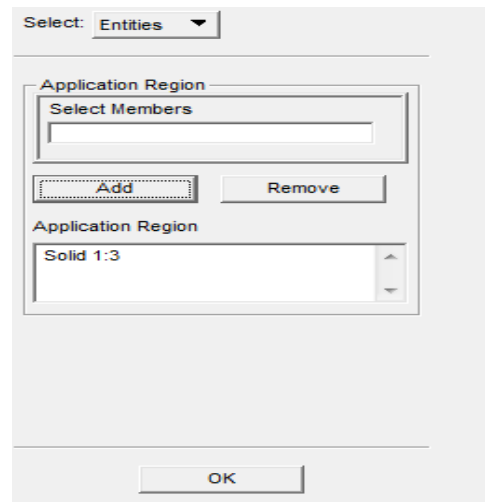


Figure 3.30: Input data for application region

Then, click the ANALYSIS part. In this part all the parameter for analysis will be set up before run the analysis. The method must be changed into analysis deck same as shown in Figure 3.31. Then, give a name to the job name part same as shown in Figure 3.31. After that, click job parameter and fill all the data needed. Firstly, click solver to get same as Figure 3.32 and then click non-positive definite.

For further analysis, select load step creation and then change the load step name. After that, click at solution parameter and tick at follower forces. Then, select load increment parameter and fill the number of step of output to 50 that shown in Figure 3.33. Select iteration parameter and change the value of relative residual force to 0.001 that shown in Figure 3.34. Then click OK for the entire event. Select load step selection and take the load step needed same as Figure 3.35. Lastly, run the analysis using CMD command to get the result of this project. After get the result, change the action at ANALYSIS part into read result and select the result file to take the result same as shown in Figure 3.36. Then, apply the result.

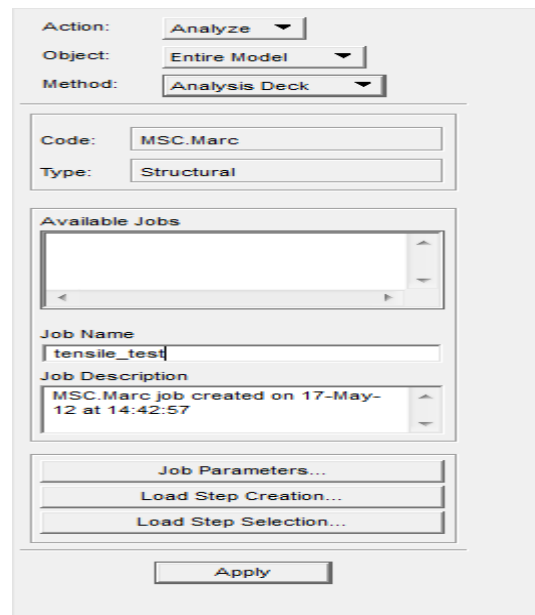


Figure 3.31: The analysis part in PATRAN software

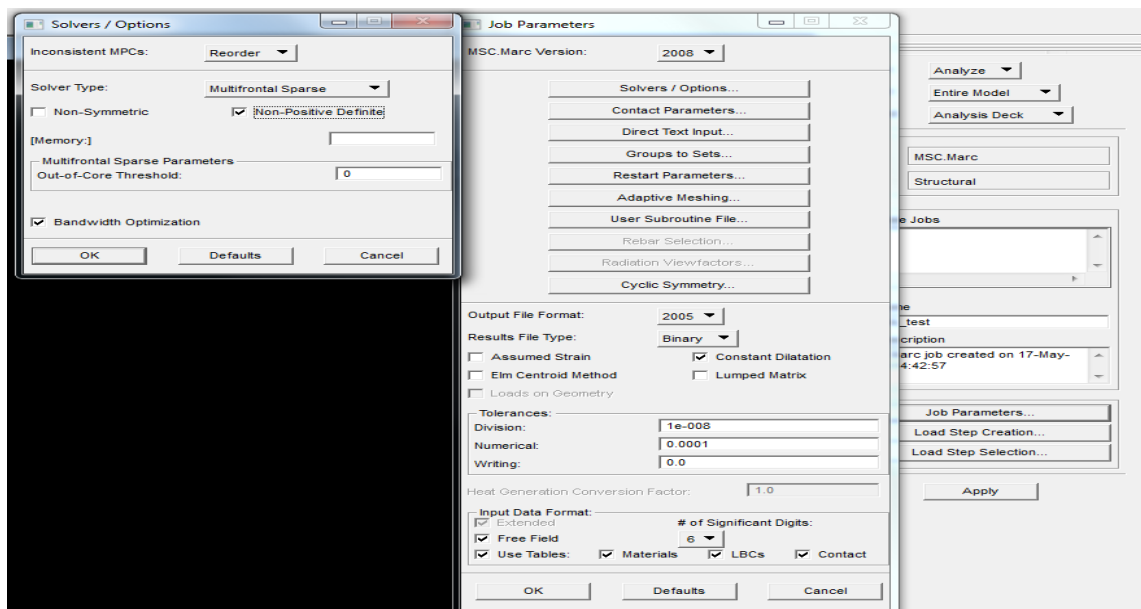


Figure 3.32: The step in job parameter part

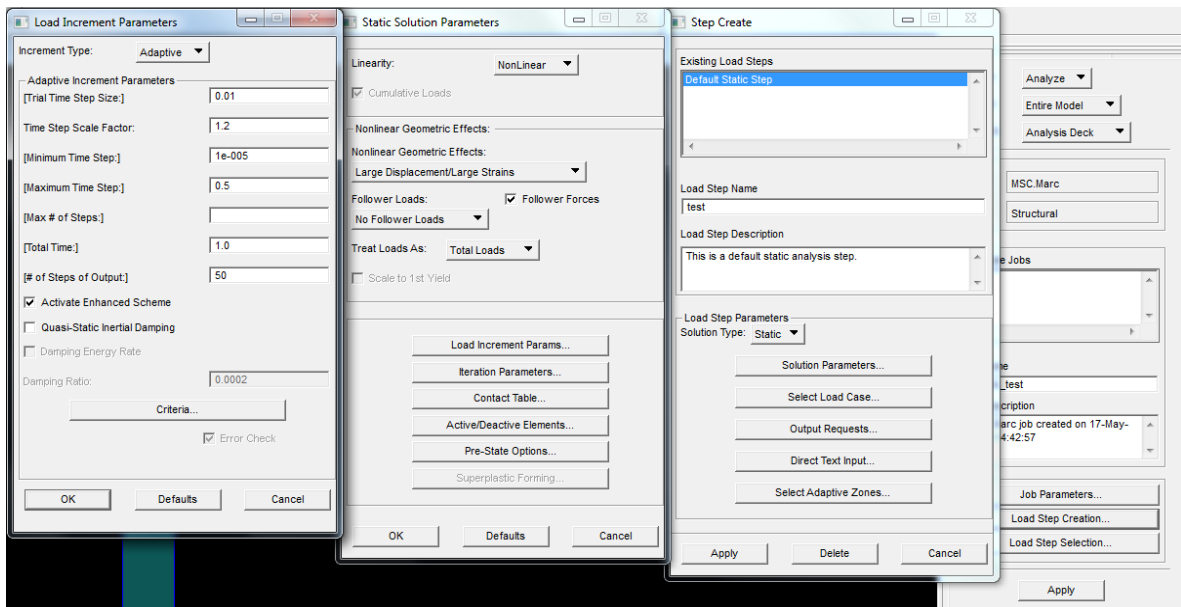


Figure 3.33: Step in load step creation part to set the load increment parameter

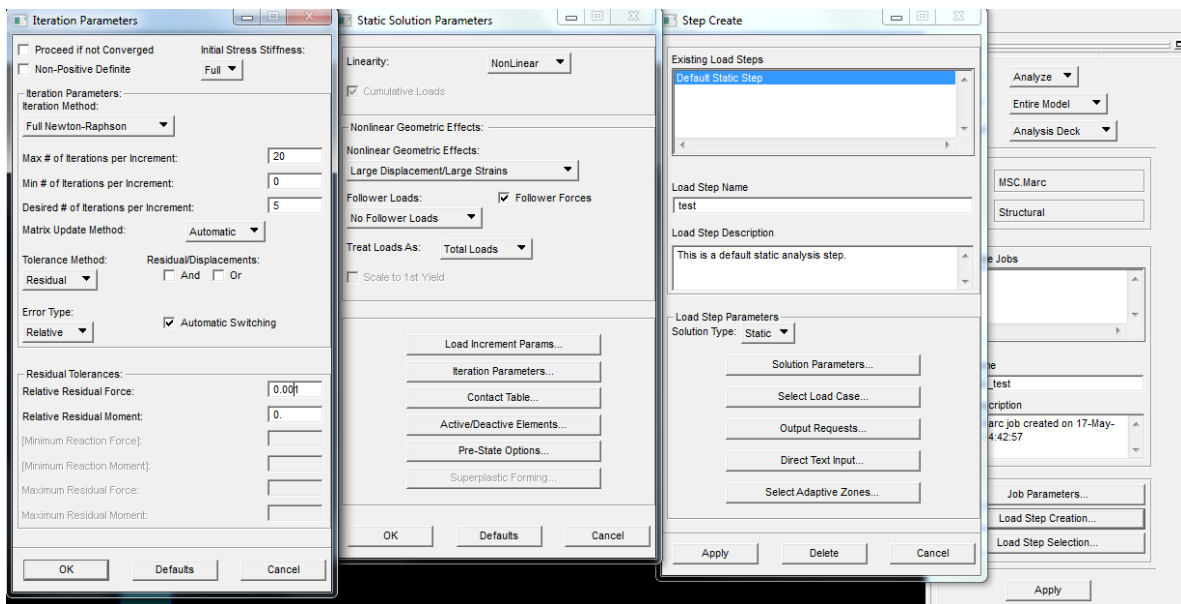


Figure 3.34: Step in load step creation part to set the iteration parameter

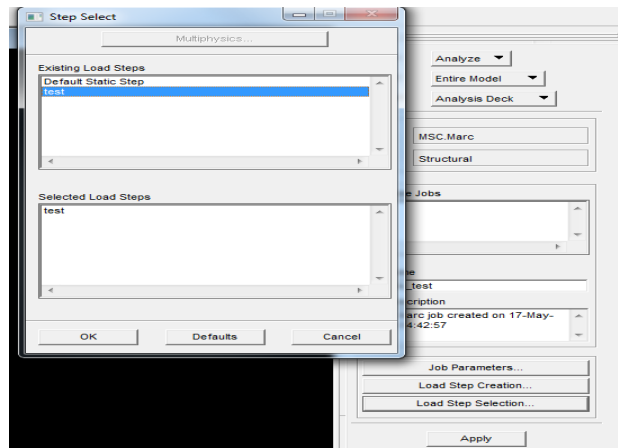


Figure 3.35: The step for load step selection

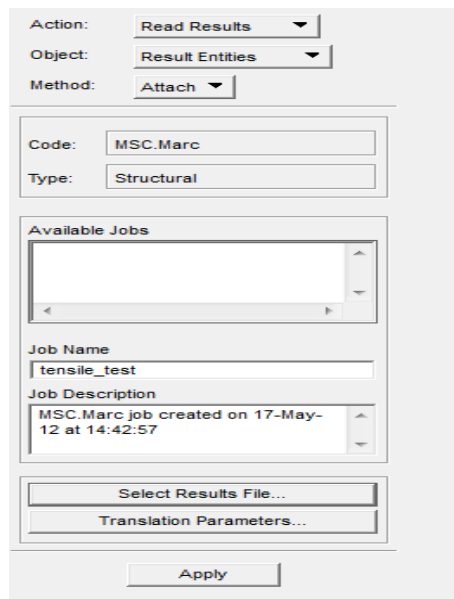


Figure 3.36: The step to read the result

The last process for Patran 2008r1 software is selecting the RESULT to read and see the result of simulation of the specimen. After run this specimen, go to result to play the movement animation to represent the displacement force in Y-direction. If the simulation don't have any problem and suitable with experiment result, next step is to take an important data for finite element analysis result.

Select all time step in the result area and take stress and strain to plot a graph in finite element analysis to make sure the simulation analysis is successful. Next, take the suitable data in RESULT part such as the data for fracture strain and stress triaxiality. Lastly, the data has been put in EXCEL and the graph needed has been plotted.

CHAPTER 4

RESULT AND DISCUSSION

4.1 INTRODUCTION

Results from the experiment and finite element analysis were presented in this chapter. All the data and result from the experiment and finite element analysis will be systematically discussed in this chapter.

The experimental result, finite element analysis (FEA) result, ductile fracture strain and stress triaxiality result were discussed in this chapter. For experiment result, engineering stress strain graph was obtained from tensile test experiment. After that, the graph should be converted into true stress strain graph to simplify the graph into true plastic stress strain graph. In this experimental result also discussed the result of every zone by doing a measurement and calculation using suitable equation that discussed in this chapter.

4.2 EXPERIMENT RESULT

This experimental result is very important and useful those needs to combine with finite element analysis (FEA) result to achieve the objective of this study. Furthermore, the result is taken from uniaxial tensile test by using SHIMADZU machine and this result will become to be an experimental result. All the result will be compiled and discussed with suitable explanation.

4.2.1 Engineering Stress-Strain Graph

The first result in this experiment is engineering stress-strain graph. This result will get from the tensile test result that give two graph after finish the test. Firstly is force versus displacement graph and another one is stress versus strain graph. However in this chapter, the stress versus strain graph is very important to do analysis by using finite element analysis (FEA) PATRAN.

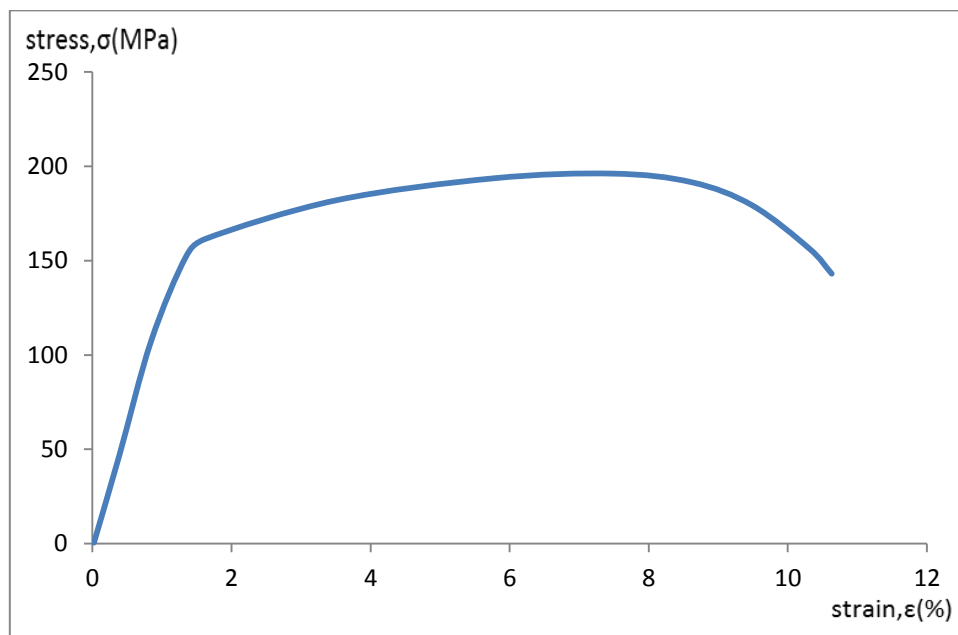


Figure 4.1: Stress versus strain curve for aluminum

Figure 4.1 shows the engineering stress-strain diagram for aluminum. Based on the graph, the maximum stress that represent as ultimate tensile strength is 195.843 MPa whereas maximum strain is 7.471 %, and maximum force is 314688.2 N. Table 4.1 indicated the mechanical properties obtained from uniaxial tensile test. In this table the value of stress and strain at the onset of fracture was also included. The stress and strain at the corresponding point is given by 143.147 MPa and 10.607 % respectively. Then the break area force is 10736.0 N.

The experimental result for aluminum in uniaxial tensile test is the lower and faster compare to others. This is because of the material strength, furthermore the aluminum is a soft material compare to others. The strength of aluminum will affect the strain value that became smaller than brass and mild steel.

Table 4.1: Mechanical properties of Aluminum obtained from tensile test

	Maximum	Break
Stress (MPa)	195.843	143.147
Strain (%)	7.471	10.607
Force (N)	314688.2	10736.0

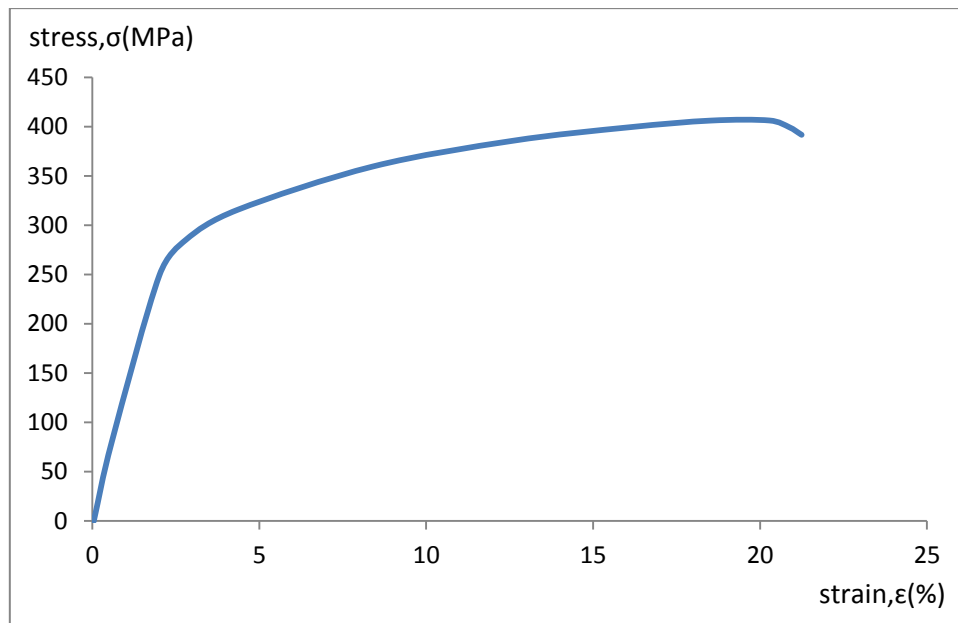


Figure 4.2: Stress versus strain curve for brass

Figure 4.2 shows the engineering stress-strain diagram for aluminum. Based on the graph, the maximum stress that represent as ultimate tensile strength is 406.885 MPa whereas maximum strain is 18.552 %, and maximum force is 30516.4 N. Table 4.2 indicated the mechanical properties obtained from uniaxial tensile test. In this table the

value of stress and strain at the onset of fracture was also included. The stress and strain at the corresponding point is given by 390.576 MPa and 21.154 % respectively. Then the break area force is 29293.2 N.

The experimental result for brass in uniaxial tensile test is higher than aluminum but lower than mild steel. This is because of the material strength, furthermore the brass is a hard and strong material compare to aluminum. The strength of brass will affect the strain value that became higher than aluminum.

Table 4.2: Mechanical properties of Brass obtained from tensile test

	Maximum	Break
Stress (MPa)	406.885	390.576
Strain (%)	18.552	21.154
Force (N)	30516.4	29293.2

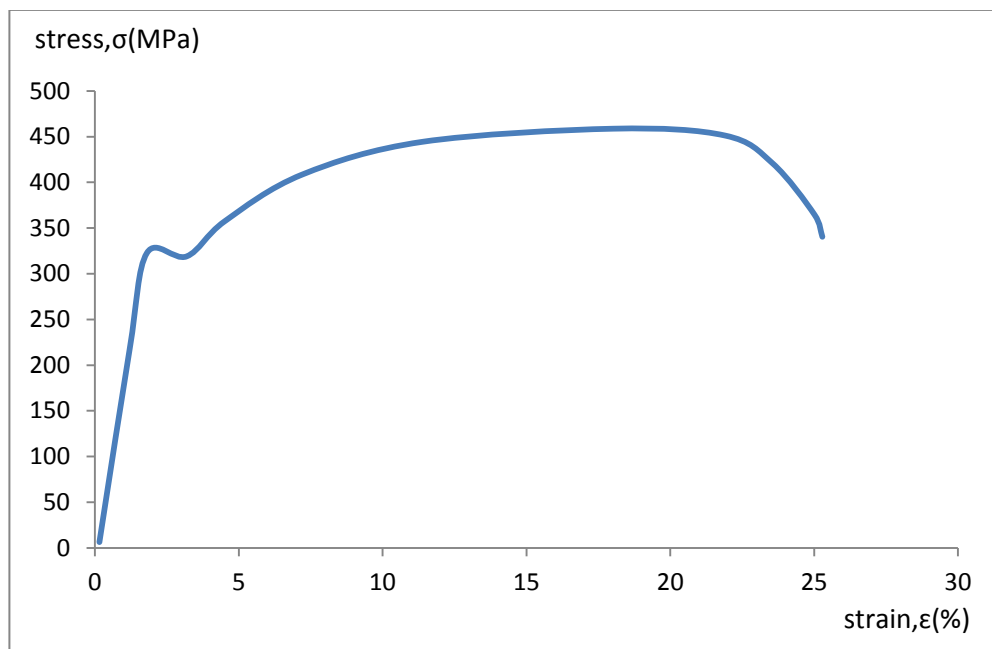


Figure 4.3: Stress versus strain curve for mild steel

Figure 4.3 shows the engineering stress-strain diagram for aluminum. Based on the graph, the maximum stress that represent as ultimate tensile strength is 456.054 MPa whereas maximum strain is 18.181 %, and maximum force is 34204 N. Table 4.3 indicated the mechanical properties obtained from uniaxial tensile test. In this table the value of stress and strain at the onset of fracture was also included. The stress and strain at the corresponding point is given by 339.037 MPa and 25.368 % respectively. Then the break area force is 25427.8N.

The experimental result for mild steel same as show in Figure 4.3 from uniaxial tensile test is the highest and strongest especially the value of maximum stress compare with others material. This is because of the material strength, furthermore the mild steel is very hard and strong material compare to aluminum and brass. The strength of mild steel obviously will affect the strain value.

Table 4.3: Mechanical properties of Mild steel obtained from tensile test

	Maximum	Break
Stress (MPa)	456.054	339.037
Strain (%)	18.181	25.368
Force (N)	34204	25427.8

4.2.2 Conversion of Engineering Stress-Strain Curve To True Stress-Strain Curve

In finite element analysis (FEA), true plastic stress-strain data must be employed as a input data for each material. Therefore, it is very important to convert engineering stress-strain data into true stress-strain data. The equations to convert engineering stress-strain into true stress-strain are given by:

$$\sigma_T = \sigma_E(\varepsilon_E + 1) \quad (4.1)$$

$$\varepsilon_T = \ln (1 + \varepsilon_E) \quad (4.2)$$

The equation 4.1 and 4.2 is only applicable up to necking point of the material. The true stress-strain data from necking point to fracture was predicted based on power law equation that is given by:

$$\sigma_T = k\varepsilon^n \quad (4.3)$$

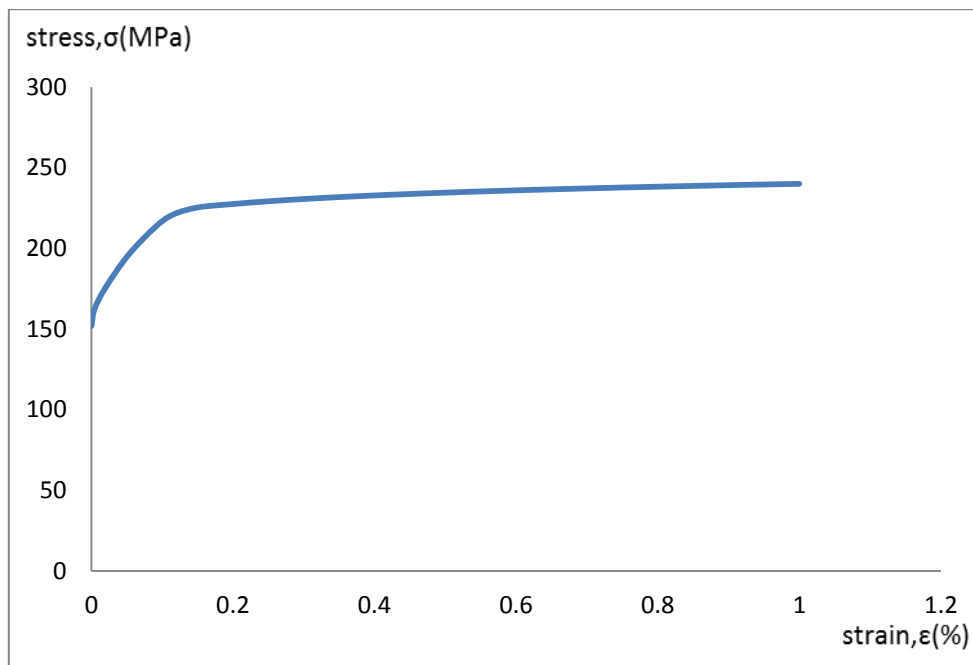


Figure 4.4: True plastic stress-strain curve for aluminum

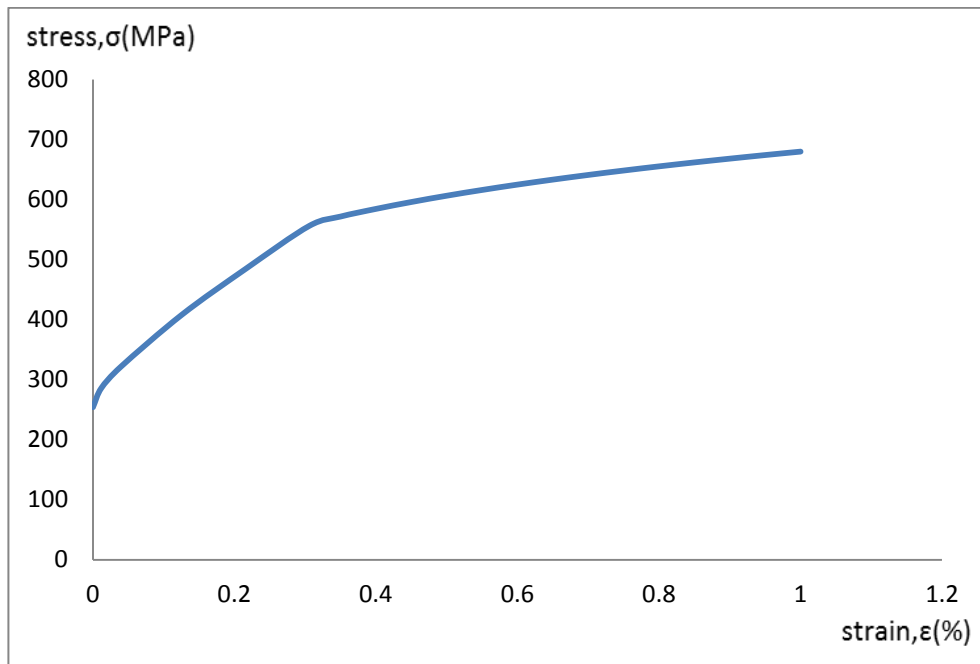


Figure 4.5: True plastic stress-strain curve for brass

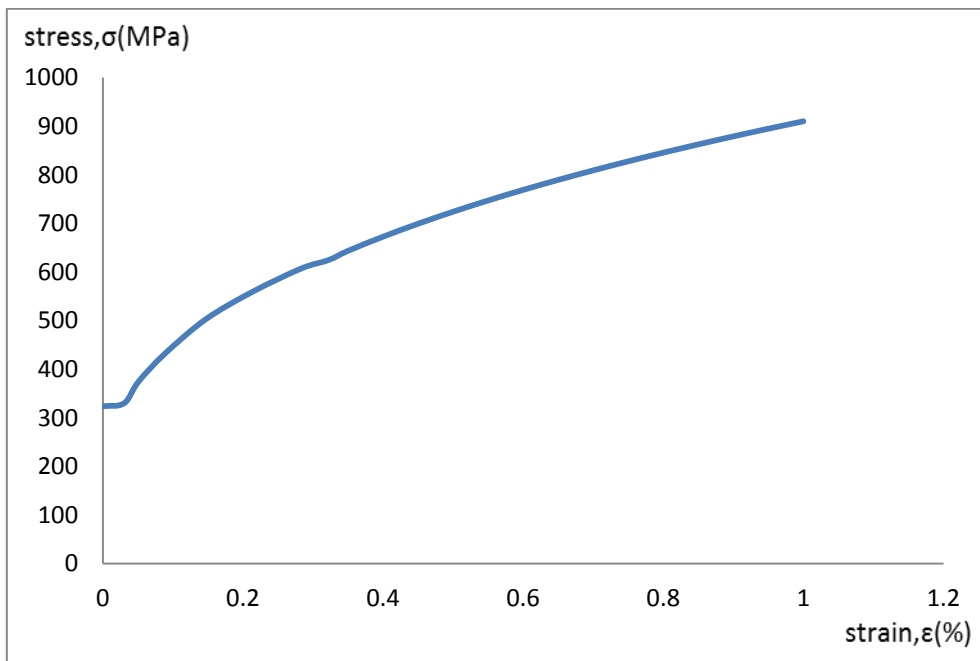


Figure 4.6: True plastic stress-strain curve for mild steel

Based on the true plastic stress-strain curve shown in Figure 4.4 to Figure 4.6, it can be concluded that the stress is increasing after the maximum point up to fracture. This is because due to the reduction of cross-section area of the material after necking was occurred.

Besides that, the pattern of these three graphs of stress-strain for aluminum, brass and mild steel are affected by the value of strain hardening coefficient and strain hardening exponent. The value of strain hardening coefficient and strain hardening exponent for each material studied are shown in Table 4.4.

Table 4.4: Mechanical properties of material tested

Material	Strain hardening coefficient, K (MPa)	Strain hardening exponent, n
ALUMINUM	240	0.033
BRASS	680	0.165
MILD STEEL	910	0.330

4.2.3 The Result For Every Zone



Figure 4.7: Failed specimen for all material. From left are aluminum, mild steel and brass.

The specimen breaks in gauge length area show in black region as show in Figure 4.7. It is true for all material tested. The break area will become smaller than before especially the thickness and width of all material.

The length of the break area was collected for every specimen by using microscope. This is because the specimens become small after the break. The length of width and thickness was obtained at the break zone. The measurement process must be done correctly to obtain the correct value. After that, the result will be collect and put in Table 4.5. Some calculation needs to do for the result of ductile fracture strain. The equation uses are:

$$\varepsilon_1 = \frac{b_1}{b_0} \quad (4.4)$$

$$\varepsilon_2 = \frac{g_1}{g_0} \quad (4.5)$$

$$\varepsilon_p = \sqrt{\frac{2}{3}} \cdot \sqrt{\varepsilon_1^2 + \varepsilon_2^2 + [-(\varepsilon_1 + \varepsilon_2)]^2} \quad (4.6)$$

Where:

b_0 = width of specimen before test

b_1 = width of specimen after test

g_0 = length of specimen before test

g_1 = length of specimen after test

$\varepsilon_1 = \varepsilon_2 = \varepsilon_p$ = plastic strain

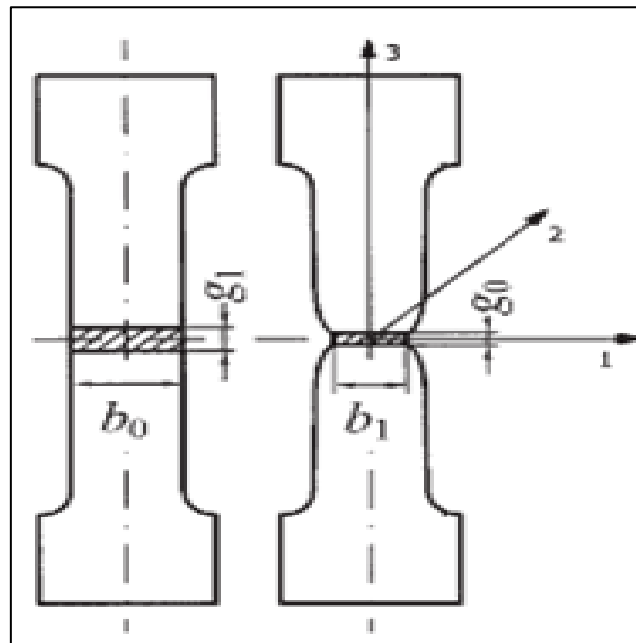


Figure 4.8: Typical tensile specimen for flat specimen

Source: Kut, 2010

The measured values of geometrical parameters in individual locations before and after the specimen tensile failure, for individual materials have been stated in Table 4.6. Then for all measured zones, the strain value ε_1 and strain value ε_2 have been calculated using equation 4.4 and 4.5, and then the ductile fracture strain values in an individual zone have been calculated using equation 4.6.

The ductile fracture strain for all material use in this study is taken from the experiment data. By using the equation 4.4 until 4.6 and refer to Figure 4.8, all data from Table 4.5 is showing that the material mild steel has the highest value of ductile fracture strain at all measuring zone compare to brass and aluminum. This is occur because of the strength of mild steel is higher than others material use. In experiment of uniaxial tensile test, it will take a long time to wait the specimen with material mild steel before it break.

Besides that, the ductile fracture strain at zone S – middle is the highest among the others measuring zones. This result occur because the value of length (thickness) of specimen after test, g_1 change very significantly. Then, the changes of width of specimen effect the value of ductile fracture strain but not very significantly compare with the changes occur by the length (thickness) of specimen. After that, these are two major reasons that affect the result of ductile fracture strain for experiment.

Table 4.5: Experimental result for ductile fracture strain

Material	Zone L,P - Lateral	Zone S - Middle
Aluminum	0.905	0.983
Brass	0.353	0.406
Mild steel	0.948	1.225

Table 4.6: Specimen's geometry and average strain values in analyzed regions

Material	Designation of parameter		Measuring zone		
			L,P lateral	S middle	C total
Aluminum	Values of geometrical parameters (mm)	g_0	6	6	6
		b_0	2.18	2.05	12.5
		g_1	3.32	2.70	3.18
		b_1	1.62	1.86	9.49
	Plastic strain	ε_1	-0.297	-0.097	-0.275
		ε_2	-0.592	-0.799	-0.635
		ε_p	0.905	0.983	0.934
Brass	Values of geometrical parameter (mm)	g_0	6	6	6
		b_0	1.89	2.11	12.5
		g_1	4.92	4.70	4.90
		b_1	1.62	1.80	10.27
	Plastic strain	ε_1	-0.154	-0.159	-0.197
		ε_2	-0.198	-0.244	-0.203
		ε_p	0.353	0.406	0.399
Mild steel	Values of geometrical parameter (mm)	g_0	6	6	6
		b_0	2.40	1.96	12.5
		g_1	3.50	2.86	3.34
		b_1	1.60	1.22	8.59
	Plastic strain	ε_1	-0.405	-0.474	-0.375
		ε_2	-0.539	-0.741	-0.586
		ε_p	0.948	1.225	0.969

4.3 FINITE ELEMENT ANALYSIS (FEA) RESULT

The results of finite element analysis are used to simplify working process and reduce working time to do an experiment. Furthermore, the result from finite element analysis usually can be used as an experiment result.

The purpose of the simulation is to indicate the area, where the state of stress on the tensioned specimen is the closest to uniaxial tension. In finite element analysis (FEA), the specimens are drawing in four quarter to simplify and minimize the specimen before run by using MSC MARC.

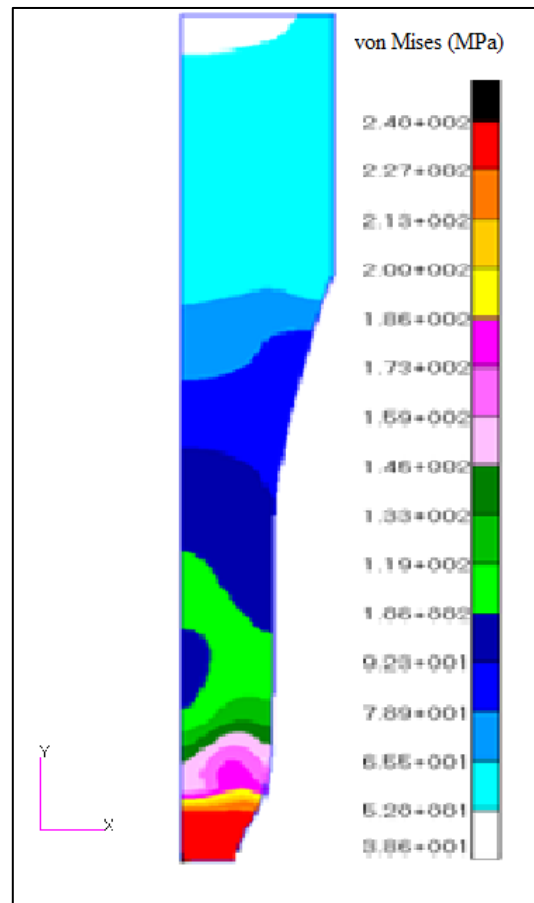


Figure 4.9: The elongation of aluminum in finite element analysis.

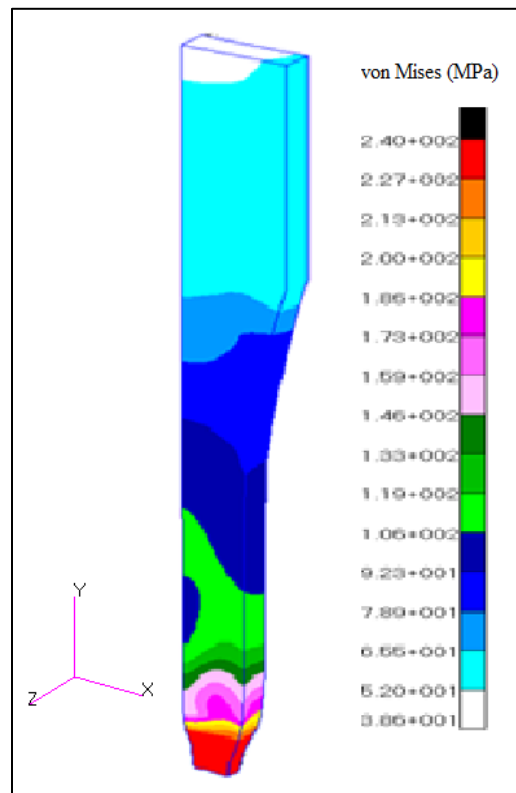


Figure 4.10: The simulation result for aluminum in 3D view.

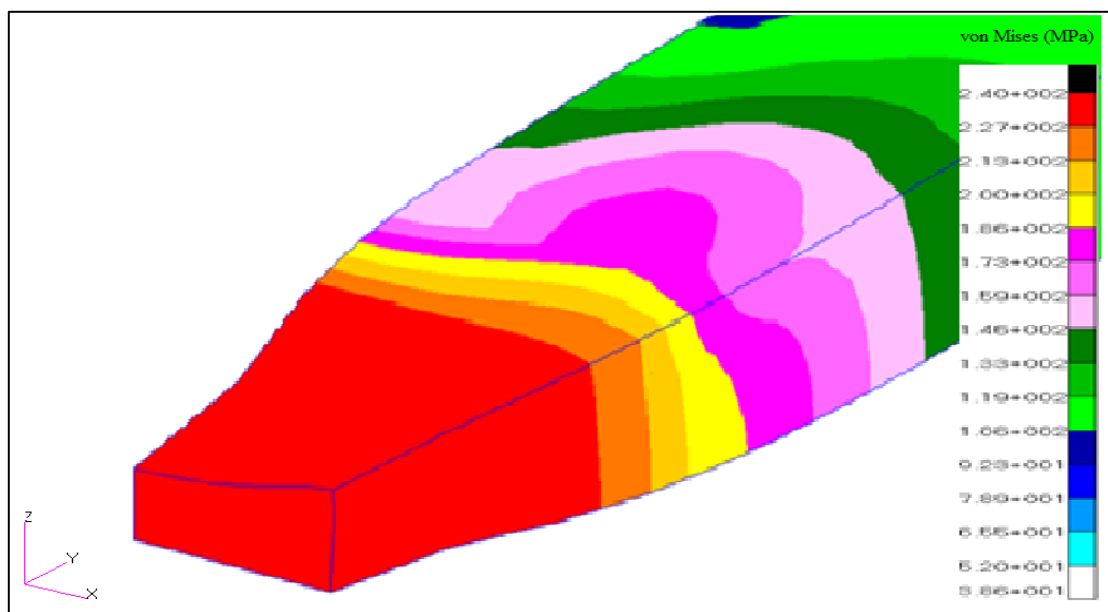


Figure 4.11: The shape of saddle at the break point for aluminum.

The colour contour represents in Figure 4.9 and Figure 4.10 is a movement of stress at this specimen in each element mesh, this happen because of apply displacement at Y-direction upward for 15 mm while in the other side of specimen is set fix with boundary condition in Y-direction downward. So the force focus in the middle of the specimen with the specimen shape is like plane dog-bone.

The red contour area represent as the highest stress apply at that area. The highest stress appear at middle of the specimen because the length of material is symmetry from one side with others side. So the elongation of specimen start from middle area and stress will focus at this area until these area break after apply displacement at Y-direction.

The result of simulation from Figure 4.9 and Figure 4.10 show the pattern of specimen simulation for aluminum when it become fracture and break. The elongation of this simulation we can see is very small that is about 8 mm displacement in Y-direction upward. The discussion for this result is because aluminum is a soft material. The aluminum strength is very low and small plastic material in aluminum compare with others.

From the figure 4.11, it focuses to the break area that show red colour of contour for aluminum. It represents that after break the shape at the break area become shape of saddle, same shape as the experimental result of uniaxial tensile test. The shape changes for aluminum at break area or study location is very small compare with others because of stress apply at this material is lower than others.

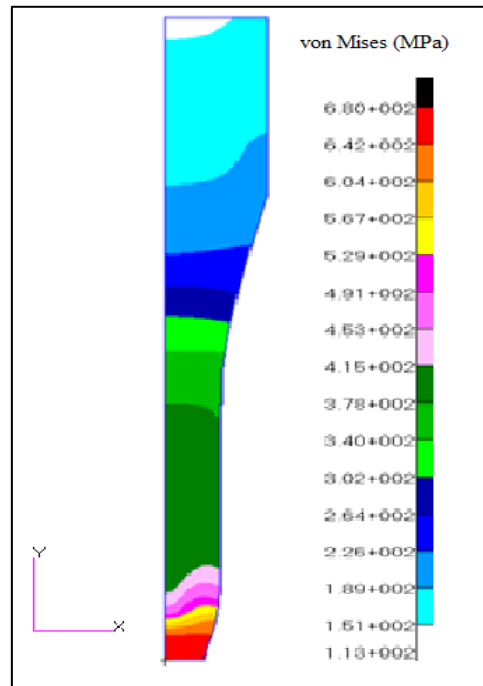


Figure 4.12: The elongation of brass in finite element analysis.

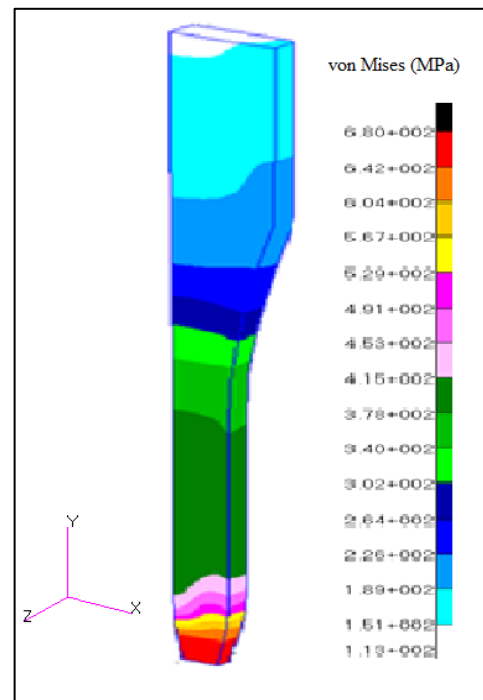


Figure 4.13: The simulation result for brass in 3D view

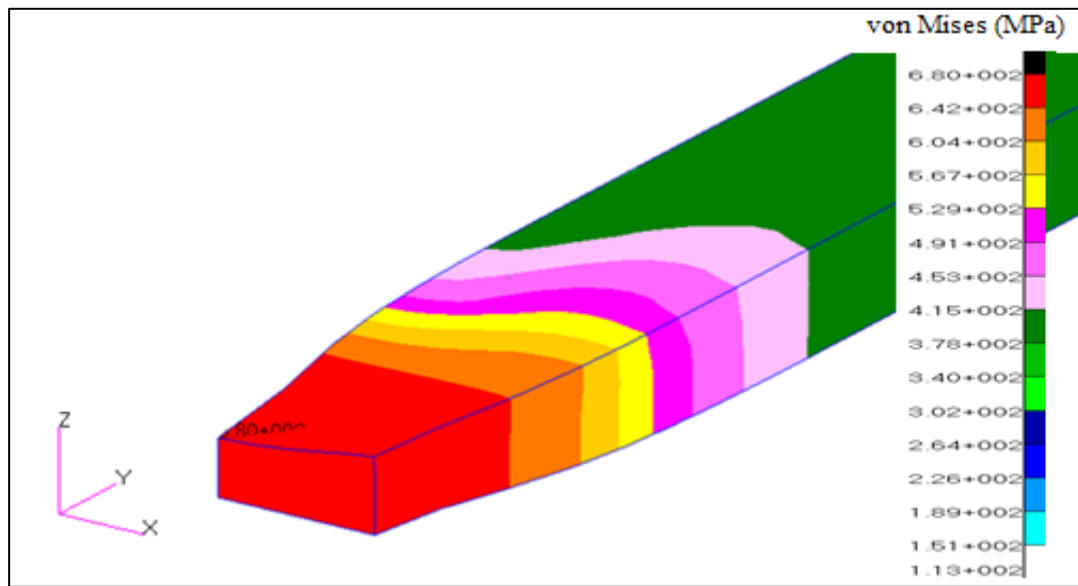


Figure 4.14: The shape of saddle at the break point for brass

The colour contour represents in Figure 4.12 and Figure 4.13 is a movement of stress at this specimen in each element mesh, this happen because of apply displacement at Y-direction upward for 15 mm while in the other side of specimen is set fix with boundary condition in Y-direction downward. So the force focus in the middle of the specimen with the specimen shape is like plane dog-bone.

The red contour area represent as the highest stress apply at that area. The highest stress appear at middle of the specimen because the length of material is symmetry from one side with others side. So the elongation of specimen start from middle area and stress will focus at this area until these area break after apply displacement at Y-direction.

The result of simulation from Figure 4.12 and Figure 4.13 show the pattern of specimen simulation for brass when it become fracture and break. The elongation of this simulation we can see is higher than aluminum that is about 11 mm displacement in Y-direction upward. The discussion for this result is because brass is more hard material compare with aluminum. The brass strength is higher and more plastic material in brass compare with aluminum.

From the figure 4.14, it focuses to the break area that show red colour of contour for brass. It represents that after break the shape of the break area become shape of saddle, same shape as the experimental result of uniaxial tensile test. The shape changes for brass at break area or study location is more higher compare with aluminum because of stress apply at this material is higher than aluminum but lower than mild steel.

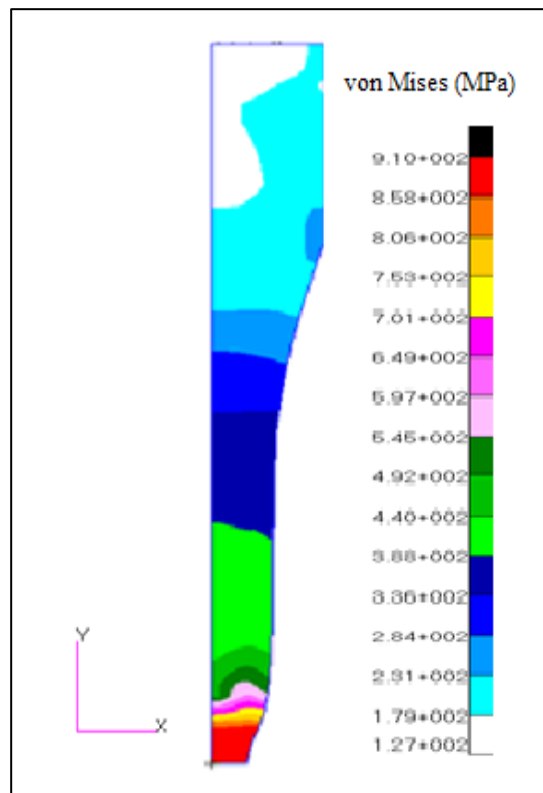


Figure 4.15: The elongation of mild steel in finite element analysis.

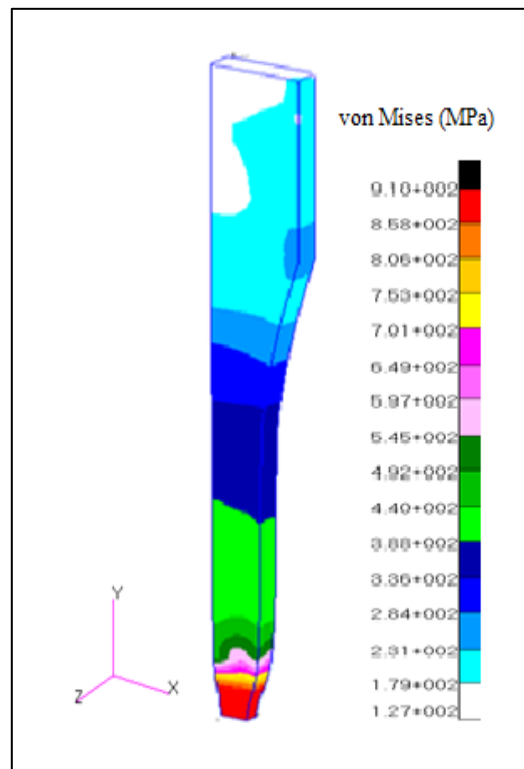


Figure 4.16: The simulation result for mild steel in 3D view.

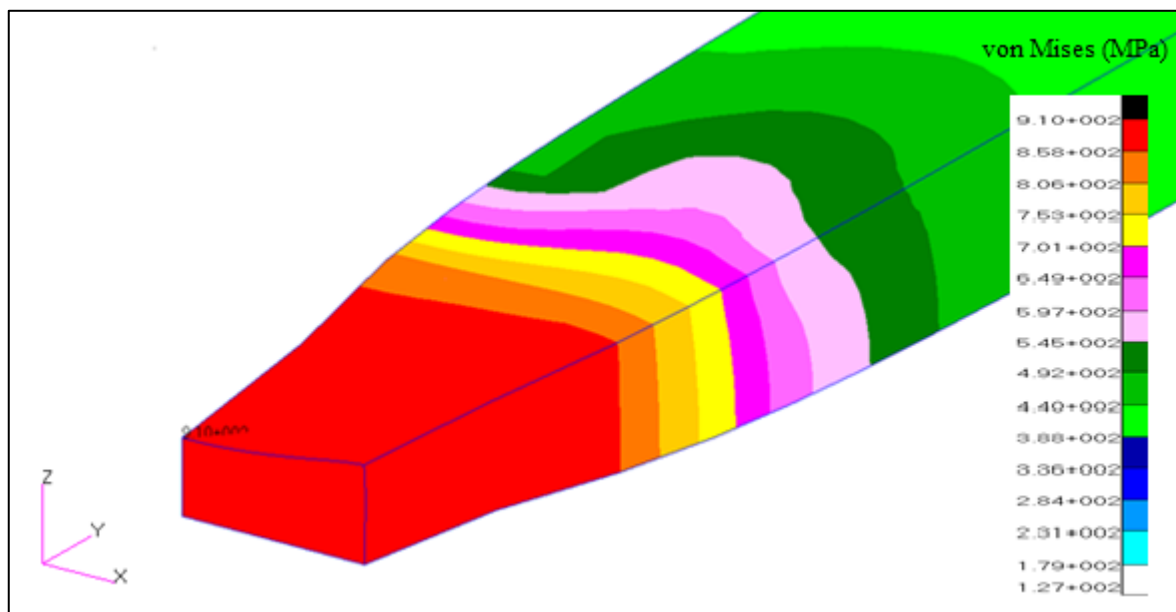


Figure 4.17: The shape of saddle at the break point for mild steel.

The colour contour represents in Figure 4.15 and Figure 4.16 is a movement of stress at this specimen in each element mesh, this happen because of apply displacement at Y-direction upward for 15 mm while in the other side of specimen is set fix with boundary condition in Y-direction downward. So the force focus in the middle of the specimen with the specimen shape is like plane dog-bone.

The red contour area represent as the highest stress apply at that area. The highest stress appear at middle of the specimen because the length of material is symmetry from one side with others side. So the elongation of specimen start from middle area and stress will focus at this area until these area break after apply displacement at Y-direction.

The result of simulation from Figure 4.15 and Figure 4.16 show the pattern of specimen simulation for mild steel when it become fracture and break. The elongation of this simulation we can see is the highest between aluminum and brass that is about 14 mm displacement in Y-direction upward. The discussion for this result is because mild steel is the hardest material compare with others. The mild steel strength is very highest and the most plastic material in mild steel compare with aluminum and brass.

From the figure 4.17, it focuses to the break area that show red colour of contour for mild steel. It represents that after break the shape of the break area become shape of saddle, same shape as the experimental result of uniaxial tensile test. The shape of mild steel changes at break area or study location is the highest compare with others because of stress apply at this material is the most highest between aluminum and brass.

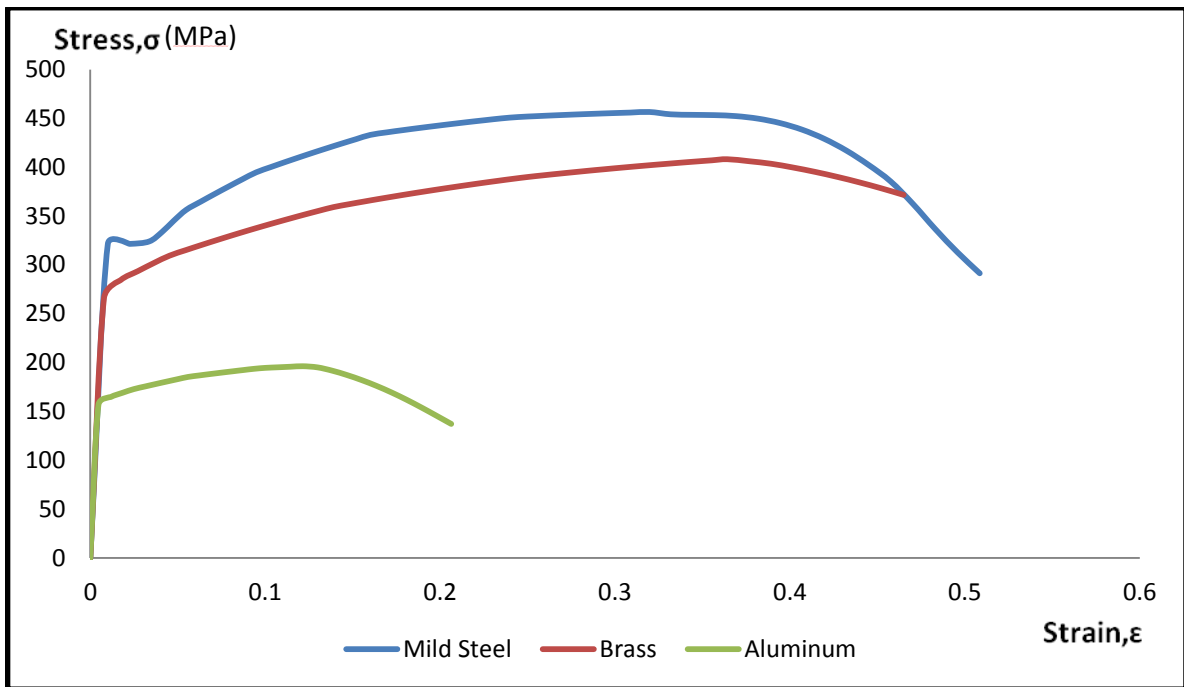


Figure 4.18: The comparison of engineering stress-strain data obtained from finite element analysis for different materials

In this case, the difference material have different stress-strain graph that got from finite element analysis (FEA). Mild steel stress-strain diagram show the highest stress and strain result which is maximum stress at range of 450 MPa while fracture strain occur in range of 0.5. Then, the value of maximum stress is in range of 410 MPa for brass and 200 MPa for aluminum. Besides that, the fracture strain for brass is in range of 0.46 and for aluminum is in range of 0.2.

The pattern and shape of graphs show in Figure 4.18 is followed the correct data that insert in the PATRAN software especially the elastic and plastic region data. For elastic region data the important part of data is the material young modulus and poisson ratio. Besides that, the plastic region data is collected from true stress-strain graph data's by using the power law equation that contains strain hardening coefficient and strain hardening exponent as shown in Table 4.4 to get the excellent result for finite element analysis (FEA) as Figure 4.18.

The overall data that represent in table mention about Strain hardening coefficient, K in unit of Mega Pascal for difference specimen material that are used in this study. The value of strain hardening coefficient for mild steel is 910 MPa that represent as the highest value compare to others material. The strain hardening coefficient, K value for aluminum is 240 MPa represent the lowest value while strain hardening coefficient, K value for brass is 680 MPa.

After that, table also shows the strain hardening exponent, n for every material that is mild steel, brass and aluminum. Mild steel has the highest value of strain hardening exponent, n that is $n = 0.33$. Then, strain hardening exponent, n for brass is $n = 0.165$, while aluminum has the lowest with $n = 0.033$.

4.4 DUCTILE FRACTURE STRAIN

The ductile fracture strain is the main result needed in this project study. Firstly, the time step that fracture occur need to know. The time step occur can be get from result part in finite element analysis and then compare the result with experimental engineering stress-strain result. Take the nearest time step with actual time fracture occurs in experiment.

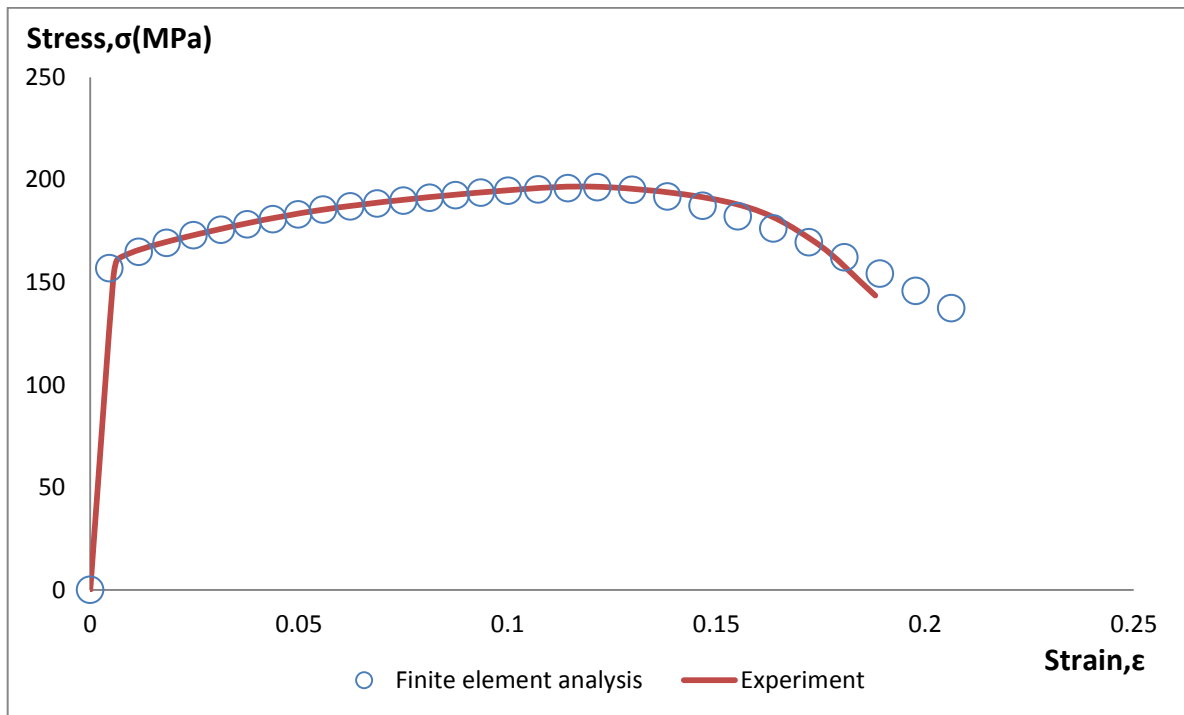


Figure 4.19: Comparison of stress-strain curve between experiment data and finite element result for aluminum.

Figure 4.19 compares the result of engineering stress-strain curve between experiment data and finite element result for aluminum. From that figure, the maximum stress is in average of 200 MPa for both experiment and finite element analysis points. The fracture point of the model can be determined by combining these two graphs. The nearest fracture point for aluminum is at time step 0.36.

After that, from the graph the actual ductile fracture strain can be measure. Take the actual data for ductile fracture strain from finite element analysis and define the suitable nodes where the stress triaxiality near to $k=0.33$ occur for aluminum.

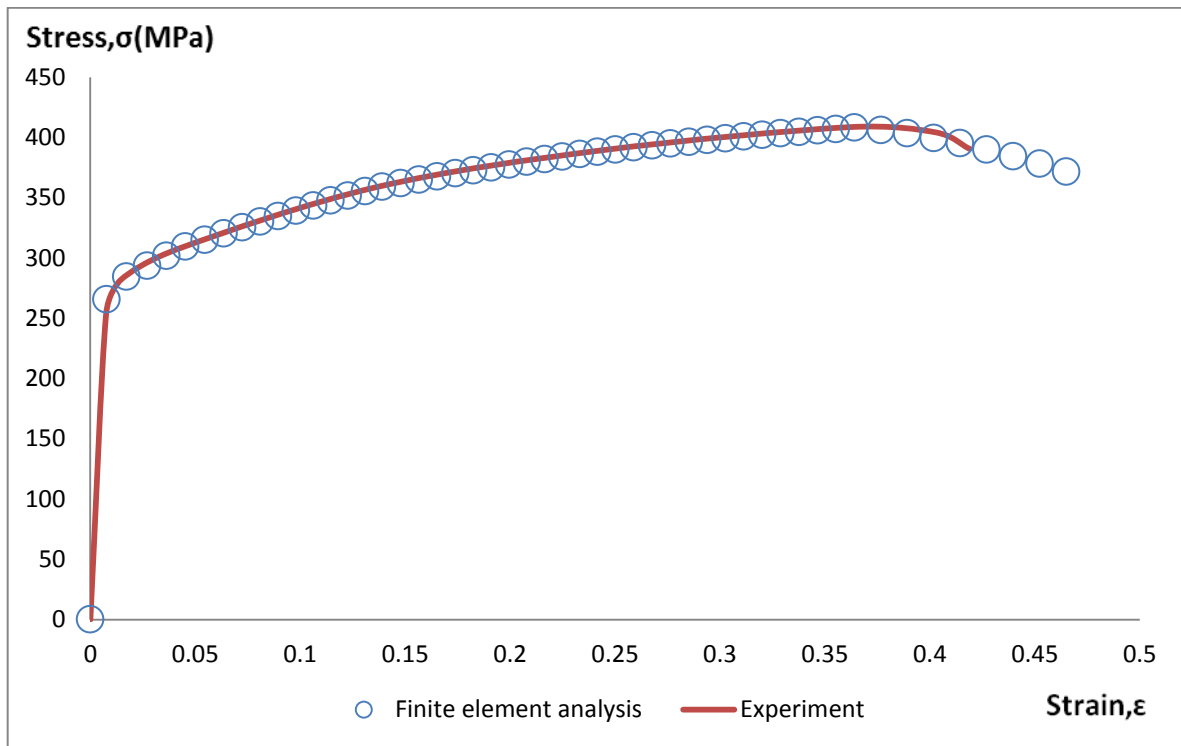


Figure 4.20: Comparison of stress-strain curve between experiment data and finite element result for brass.

Figure 4.20 compares the result of engineering stress-strain curve between experiment data and finite element result for brass. From that figure, the maximum stress is in average of 420 MPa for both experiment and finite element analysis points. The fracture point of the model can be determined by combining these two graphs. The nearest fracture point for brass is at time step 0.92.

After that, from the graph the actual ductile fracture strain can be measure. Take the actual data for ductile fracture strain from finite element analysis and define the suitable nodes where the stress triaxiality near to $k=0.33$ occur for brass.

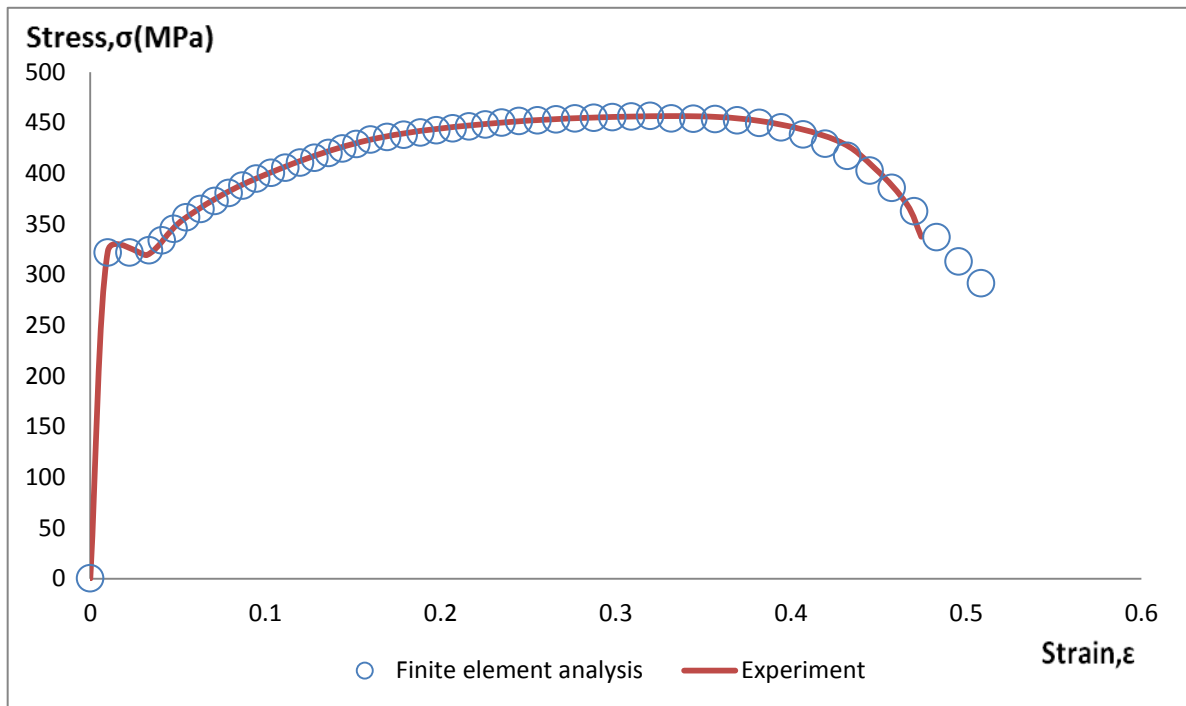


Figure 4.21: Comparison of stress-strain curve between experiment data and finite element result for mild steel.

Figure 4.21 compares the result of engineering stress-strain curve between experiment data and finite element result for mild steel. From that figure, the maximum stress is in average of 450 MPa for both experiment and finite element analysis points. The fracture point of the model can be determined by combining these two graphs. The nearest fracture point for mild steel is at time step 0.96.

After that, from the graph the actual ductile fracture strain can be measure. Take the actual data for ductile fracture strain from finite element analysis and define the suitable nodes where the stress triaxiality near to $k=0.33$ occur for mild steel.

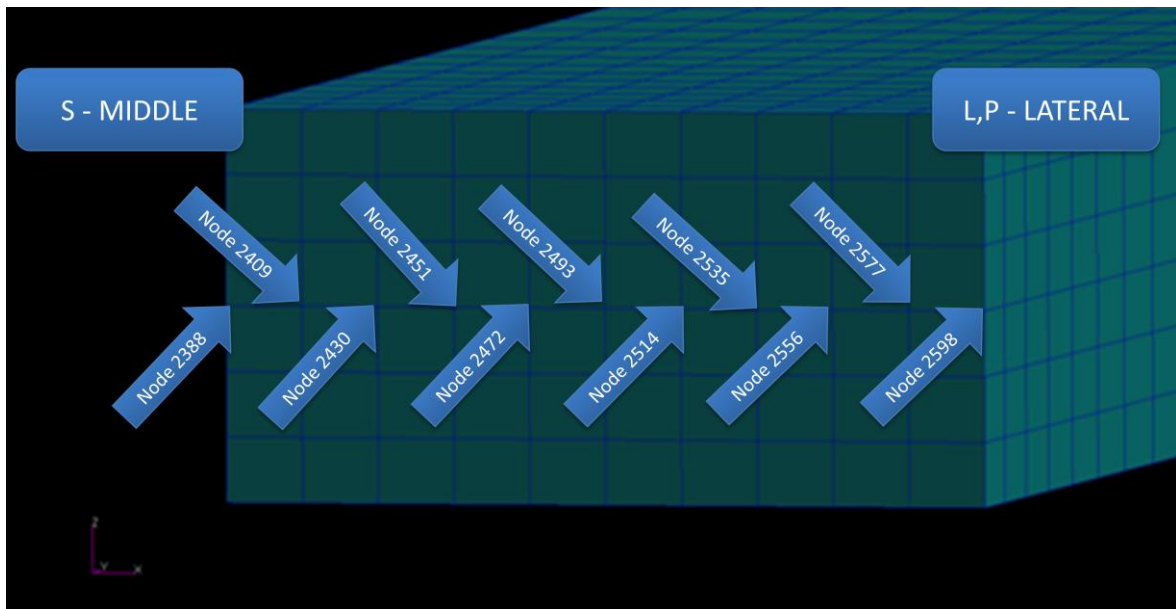


Figure 4.22: Study nodes location in Finite Element Analysis (FEA)

The break area of specimen is a study location where the necking and fracture occur here. In this project study, the mesh is divided into eleven nodes to investigate the suitable and nearest node to stress triaxiality is 0.33 for actual value of uniaxial tensile test.

From Figure 4.22 represents there are two main areas needed to study those are L, P-lateral zone and S-middle zone of the specimen. The lateral area represent as node 2598 while at middle area represent as node 2388. Then, there are another nine nodes in range between lateral and middle. The number of nodes for all these nine zones are represent in Figure 4.22.

After that, plot a graph of stress triaxiality versus time step for every node to get the suitable node to find the actual ductile fracture strain value. The stress triaxiality data can get from finite element analysis software that is PATRAN 2008r1 software.

4.5 STRESS TRIAXIALITY

Stress triaxiality is mean normal stress divide by equivalent stress. There is an equation to get stress triaxiality from finite element analysis (FEA) in PATRAN 2008r1 software. The equation use is show below:

$$\text{stress triaxiality, } k = \frac{(\sigma_1 + \sigma_2 + \sigma_3)/3}{\sqrt{(\sigma_1 - \sigma_2)^2 + (\sigma_2 - \sigma_3)^2 + (\sigma_1 - \sigma_3)^2}/2} \quad (4.7)$$

The equation 4.7 was used to determine the stress triaxiality for each material. Data for every node was collected in order to compare the result of stress triaxiality that the uniaxial ductile fracture strain occurred.

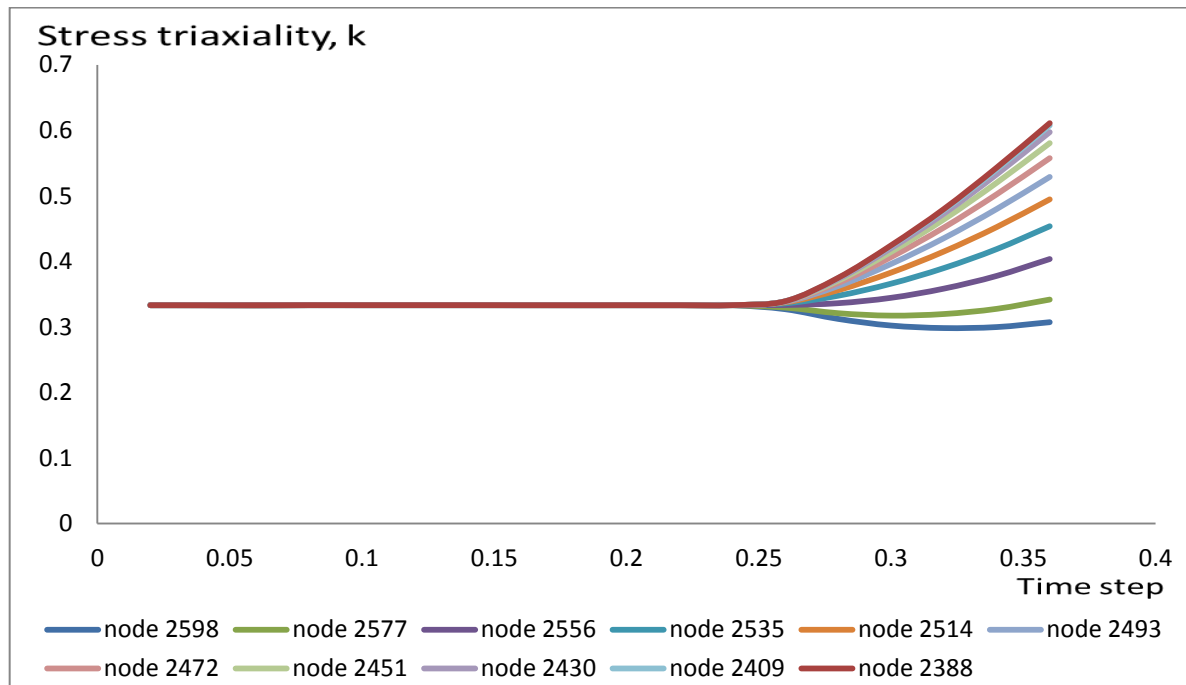


Figure 4.23: The comparison of stress triaxiality for aluminum in different zones:

L, *P*-lateral, *S*-middle and all study nodes.

Figure 4.23 above, it shows the patterns of graph stress triaxiality versus time step where the aluminum specimen fracture strain occur. There are difference results for every study node because after the specimens achieve maximum tensile strength the entire node stress triaxiality increasing near to become biaxial tension.

The state of stress factor k distribution in the initial and final phase of the specimen tensile test has been presented on Figure 4.23 for material aluminum. The state of stress triaxiality in the lateral zone L and P changes slightly in the uniaxial tension direction that is reaching $k = 0.307$ in its final phase. Besides that, the state of stress triaxiality in the middle zone S changes significantly in the biaxial tension direction that is reaching $k = 0.611$ in its final phase.

After that, the result of stress triaxiality at the time step 0.36 where the fracture occur for aluminum that show in Figure 4.23 are put in Table 4.7. From that table, the suitable node where the stress triaxiality value near 0.33 is at node 2577 where the result of stress triaxiality is 0.342 for aluminum. So, to get the uniaxial ductile fracture strain for aluminum this node 2577 must be referred.

Table 4.7: The stress triaxiality at every node for aluminum specimen

Node	2598	2577	2556	2535	2514	2493	2472	2451	2430	2409	2388
Stress Triaxiality	0.307	0.342	0.404	0.454	0.495	0.529	0.558	0.581	0.597	0.608	0.611

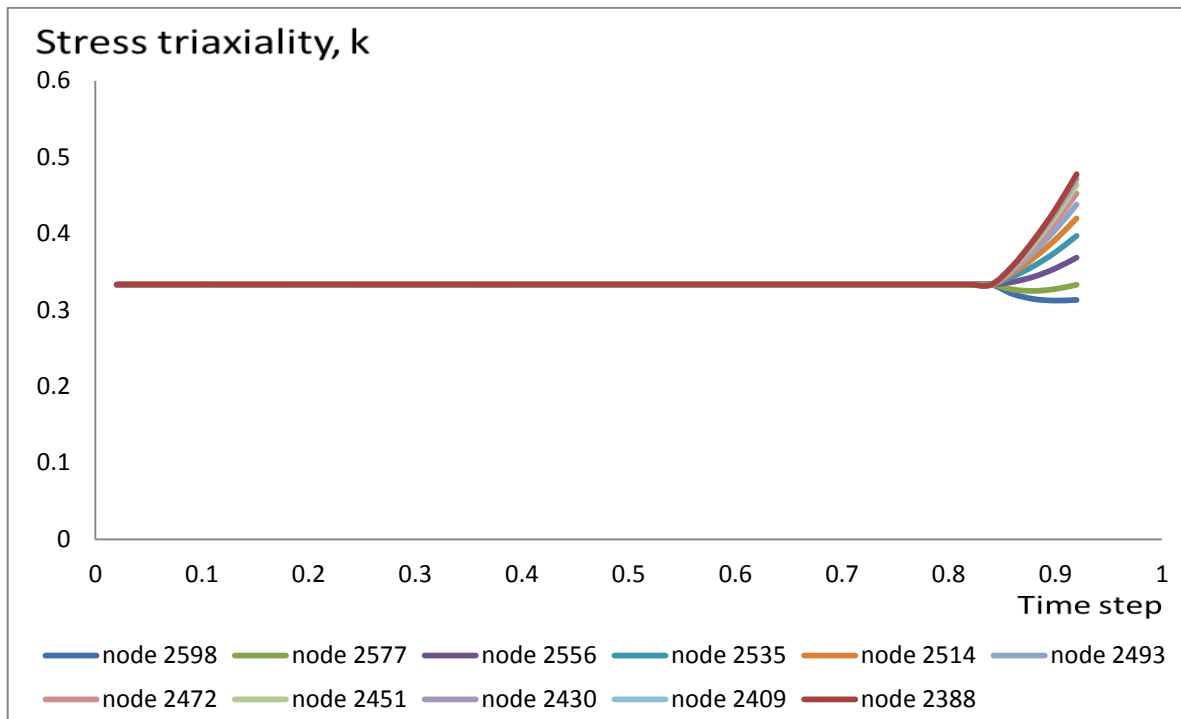


Figure 4.24: The comparison of stress triaxiality for brass in different zones: *L*, *P*-lateral, *S*-middle and all study nodes.

From the Figure 4.24 above, it shows the patterns of graph stress triaxiality versus time step where the brass specimen fracture strain occur. There are difference results for every study node because after the specimens achieve maximum tensile strength the entire node stress triaxiality increasing near to become biaxial tension.

The state of stress factor k distribution in the initial and final phase of the specimen tensile test has been presented on Figure 4.24 for material brass. The state of stress triaxiality in the lateral zone *L* and *P* changes slightly in the uniaxial tension direction that is reaching $k = 0.313$ in its final phase. Besides that, the state of stress triaxiality in the middle zone *S* changes significantly in the biaxial tension direction that is reaching $k = 0.477$ in its final phase.

After that, the result of stress triaxiality at the time step 0.92 where the fracture occur for brass that show in Figure 4.24 are put in Table 4.8. From that table, the suitable node where the stress triaxiality value near 0.33 is at node 2577 where the result of stress triaxiality is 0.333 for brass. So, to get the uniaxial ductile fracture strain for brass this node 2577 must be referred.

Table 4.8: The stress triaxiality at every node for brass specimen

Node	2598	2577	2556	2535	2514	2493	2472	2451	2430	2409	2388
Stress Triaxiality	0.313	0.333	0.369	0.397	0.420	0.438	0.452	0.463	0.471	0.476	0.477

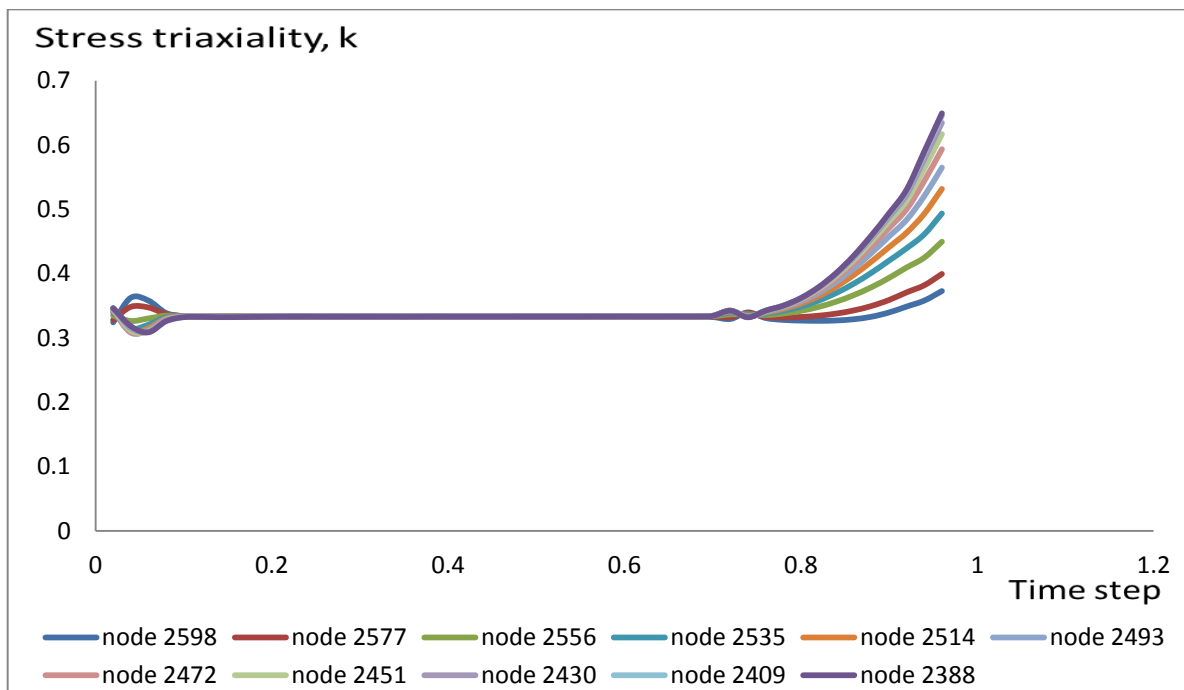


Figure 4.25: The comparison of stress triaxiality for mild steel in different zones: *L*, *P*-lateral, *S*-middle and all study nodes.

From the Figure 4.25 above, it shows the patterns of graph stress triaxiality versus time step where the mild steel specimen fracture strain occur. There are difference results for every study node because after the specimens achieve maximum tensile strength the entire node stress triaxiality increasing near to become biaxial tension.

The state of stress factor k distribution in the initial and final phase of the specimen tensile test has been presented on Figure 4.25 for material mild steel. The state of stress triaxiality in the lateral zone L and P changes slightly in the uniaxial tension direction that is reaching $k = 0.373$ in its final time step. Besides that, the state of stress triaxiality in the middle zone S changes significantly in the biaxial tension direction that is reaching $k = 0.649$ in its final time step.

After that, the result of stress triaxiality at the time step 0.96 where the fracture occur for mild steel that show in Figure 4.25 are put in Table 4.9. From that table, the suitable node where the stress triaxiality value near 0.33 is at node 2598 where the result of stress triaxiality is 0.373 for mild steel. So, to get the uniaxial ductile fracture strain for mild steel this node 2598 must be referred.

Table 4.9: The stress triaxiality at every node for mild steel specimen

Node	2598	2577	2556	2535	2514	2493	2472	2451	2430	2409	2388
Stress Triaxiality	0.373	0.399	0.449	0.493	0.532	0.565	0.593	0.616	0.634	0.645	0.649

Next, the result of actual ductile fracture strain become easier to determine when know the suitable node need to refer. Just take the data from finite element analysis of PATRAN 2008r1 software at node 2577 for aluminum and brass while at node 2598 for mild steel. The final results of ductile fracture strain for all specimens are represented in Table 4.10 until Table 4.12.

However, from the result those are represented in all table show comparison between experimental and finite element analysis result for fracture strain. But the differences between these two results are not very obvious. The finite element analysis by using PATRAN software can be used to investigate the actual ductile fracture strain in tensile test for plane specimen.

Finally, the node that are near the lateral zone L or P are the nearest area to read the ductile fracture strain value for each material in uniaxial tensile test for plane specimen. These results achieve the objective of this project study to investigate the ductile fracture strain in uniaxial tensile test for plane specimen.

From finite element analysis result at uniaxial tension region or easily say at node 2577 for aluminum uniaxial fracture strain is 0.913. Then, at node 2577 for brass specimen uniaxial fracture strain is 0.365 while at node 2598 for mild steel specimen uniaxial fracture strain is 1.025.

Table 4.10: Ductile fracture strain for aluminum at different zones

ALUMINUM			
POSITION	EXPERIMENT	FINITE ELEMENT ANALYSIS	ERROR (%)
L,P - LATERAL	0.905	0.908	0.33
S - MIDDLE	0.983	0.985	0.20
NODE 2577	-	0.913	-

Table 4.11: Ductile fracture strain for brass at different zones

BRASS			
POSITION	EXPERIMENT	FINITE ELEMENT ANALYSIS	ERROR (%)
L,P - LATERAL	0.353	0.360	1.94
S - MIDDLE	0.406	0.406	0
NODE 2577	-	0.365	-

Table 4.12: Ductile fracture strain for mild steel at different zones

MILD STEEL			
POSITION	EXPERIMENT	FINITE ELEMENT ANALYSIS	ERROR (%)
L,P - LATERAL	0.948	0.944	0.42
S - MIDDLE	1.225	1.217	0.65
NODE 2598	-	1.025	-

CHAPTER 5

CONCLUSION

5.1 CONCLUSION

The main objective of this study is to determine the uniaxial ductile fracture strain in tensile test of plane specimen. The experiments performed show that the fracture strain in the tensile test for plane specimen must be determined in L or P zone that is in lateral region, as the state of stress in these zones is nearest to the uniaxial tension. The result from simulation shows that the predicted ductile fracture strain is close to experiment result as the meshing is sufficiently small.

It is well known that the uniaxial fracture strain occurred at stress triaxiality of 0.33. In this study, uniaxial fracture strain was determined from element with stress triaxiality of 0.33 that occurred at fracture point. The result obtained from this study was shown the pattern of stress triaxiality graph versus time step was changed after the necking occurred. From the starting result until necking point, the value of stress triaxiality was obtained in uniaxial tension value. The stress triaxiality value was changed after the specimen was loaded exceed from this point. It will become to a simple shear value that is $k=0$, where the decrease for a while near to this simple shear value before it increase the stress triaxiality value to biaxial region that is near 0.66 until the ductile fracture point.

5.2 RECOMMENDATIONS

Recommendation is very important in this project because it will affect the quality of the project for future study. So, in this recommendation part there are suitable to give an opinion or suggestion about disadvantage of this study project and give a suggestion for future study improvement.

Firstly, the recommendation is for specimen preparation part. This process must be done accurately especially the specimen dimension because sometimes it will affect the result of the experiment especially the ductile fracture strain value that needs to measure and calculate. Then to measure the length and width of lateral and middle area must be use the suitable and accurate measurement tools to get a correct data.

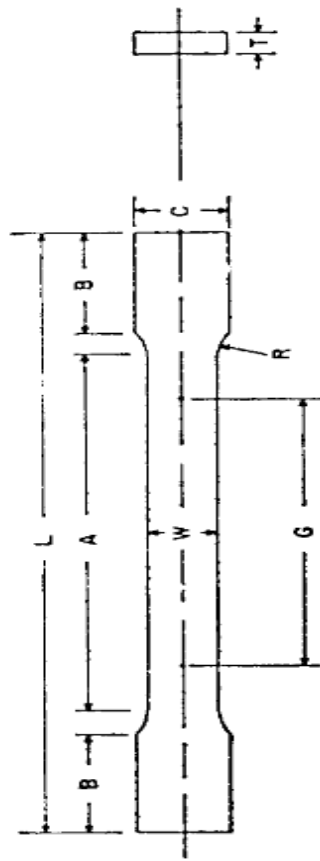
Secondly, the meshing process by using PATRAN software must be done properly because simple mesh for the specimen will be effect at the result. And also, complicated mesh will give the same result. The study area needed must be more focus mesh to get a good result. So, be careful with the specimen meshing and make sure the meshing become smooth and proper to get the best result.

REFERENCES

- Bridgman, P.W., 1952. *Studies in Large Flow and Fracture*. McGraw-Hill, New York.
- Cabezas, E.E., Celentano, D.J., 2004. Experimental and numerical analysis of the tensile test using sheet specimens. *Finite Elements in Analysis and Design* **40** (5–6): 555–575.
- Campitelli, E.N., Spatig, P., Bonade, R., Hoffelner, W., Victoria, M., 2004. Assessment of the constitutive properties from small ball punch test: experiment and modeling. *Journal of Nuclear Materials* **335** (3): 366–378.
- Choi, Y., Kim, B.M., Choi, J.C., 1997. A method of determining flow stress and friction factor by the ring compression test. In: *Proceedings of the Korean Society of Mechanical Engineering 1997 Spring Annual Meeting, Chonnam National University, Republic of Korea*, pp. 547–552.
- Choung, J.M. and Cho, S.R. 2008. Study on true stress correction from tensile tests. *Journal of Mechanical Science and Technology*. 22: 1039-1051.
- Haddadi, H., Bouvier, S., Banu, M., Maier, C., Teodosiu, C., 2006. Towards an accurate description of the anisotropic behavior of sheet metals under large plastic deformations: modelling, numerical analysis and identification. *International Journal of Plasticity* 22: 2226–2271.
- Husain, A., Sehgal, D.K., Pandey, R.K., 2004. An inverse finite element procedure for the determination of constitutive tensile behavior of materials using miniature specimen. *Computational Materials Science*. **31** (1–2): 84–92.
- Isselin, J., Iost, A., Golel, J., Najjar, D., Bigerelle, M., 2006. Assessment of the constitutive law by inverse methodology: small punch test and hardness. *Journal of Nuclear Materials*. **352** (1–3): 97–106.
- Koc, P., Stok, B., 2004. Computer-aided identification of the yield curve of a sheet metal after onset of necking. *Computational Materials Science* **31** (1–2): 155–168.
- Komori, K., 2002. Simulation of tensile test by node separation method. *Journal of Materials Processing Technology* **125–126** (9): 608–612.
- Kut, S. 2010. A simple method to determine ductile fracture strain in a tensile test of plane specimen's. *Metalurgia*. **49**(4): 295-299.
- Lee, H., Lee, J.H., Pharr, G.M., 2005. A numerical approach to spherical indentation techniques for material property evaluation. *Journal of the Mechanics and Physics of Solids* **53** (9): 2037–2069.

- Ling, Y. 1996: Uniaxial True Stress-Strain after Necking. *AMP Journal of Technology*. **5**: 37-48.
- Luo, M. 2008. Ductile fracture characterization of an aluminum alloy sheet using numerical simulations and tests. *Term Project Report of 2.094*: 1-21.
- Mahmudi, R., Mohammadi, R., and Sepehrband, P. 2004. Determination of tearing energy from uniaxial tension tests of aluminum alloy sheet. *Journal of Materials Processing Technology*. 147: 185-190.
- Mirone, G., 2004. A new model for the elastoplastic characterization and the stress-strain determination on the necking section of a tensile specimen. *International Journal of Solids and Structures* **41** (13): 3545–3564.
- Nayebi, A., Abdi, R.El., Bartier, O., Mauvoisin, G., 2002. New procedure to determine steel mechanical parameters from the spherical indentation technique. *Mechanics of Materials* **34** (4): 243–254.
- Puri, A.B. and Bhattacharyya, B. 2003. Modelling and analysis of the wire-tool vibration in wire-cut EDM. *Journal of Material Processing Technology*.141: 295-301.
- Scheider, I., Brocks, W., and Cornec, A., 2004. Procedure for the determination of true stress-strain curves from tensile tests with rectangular cross-section specimens, *Journal Engineering Materials Technology*. 126: 70-76.
- Springmann, M., and Kuna, M., 2005. Identification of material parameters of the Gurson–Tvergaard–Needleman model by combined experimental and numerical techniques. *Computational Materials Science*. **32** (3–4): 544–552.
- Zhang, K.S., 1995. Fracture prediction and necking analysis. *Engineering Fracture Mechanics* **52** (3): 575–582.
- Zhang, K.S., and Li, Z.H., 1994. Numerical Analysis of the Stress-Strain Curve and Fracture Initiation for Ductile Material, *Engineering Fracture Mechanics*. 49: 235-241
- Zhang, K.S., Hauge, M., Odegard, J., and Thaulow, C., 1999. Determining material true stress-strain curve from tensile specimens with rectangular cross section, *International Journal of Solids and Structures*. 36: 3497-3516
- Zhang, Z.L., Hauge, M., Ødegard, J., Thaulow, C., 1999. Determining material true stress-strain curve from tensile specimens with rectangular cross-section. *International Journal of Solids and Structures* **36** (23): 3497–3516.

APPENDIX A



Dimensions

Standard Specimens		Subsize Specimen
Plate-Type, 1½-in. Wide	Sheet-Type, ½-in. Wide	¼-in. Wide
in.	in.	in.
8.00 ± 0.01	2.000 ± 0.005	1.000 ± 0.003
1½ + ⅛, - ¼	0.500 ± 0.010	0.250 ± 0.005
1	thickness of material	
18	½	¼
9	8	4
3	2¼	1¼
2	2	1¼
	¾	¾

G—Gage length (Note 1 and Note 2)

W—Width (Note 3 and Note 4)

T—Thickness (Note 5)

R—Radius of fillet, min (Note 6)

L—Over-all length, (Note 2, Note 7 and Note 8)

A—Length of reduced section, min

B—Length of grip section, (Note 8)

C—Width of grip section, approximate (Note 4 and Note 9)

Figure A: the standard ASTM tensile test dimension for plane specimen

APPENDIX B

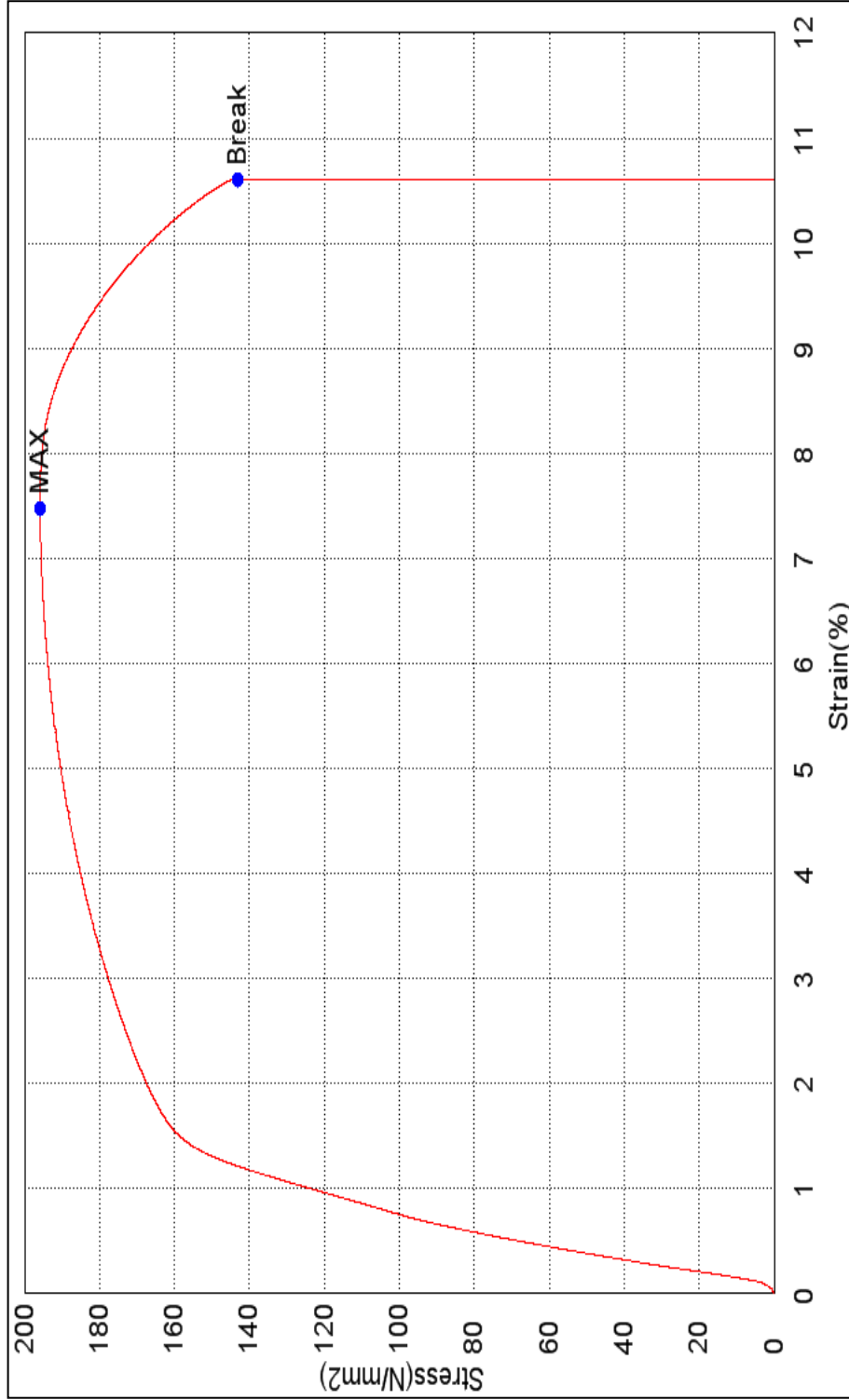


Figure B: Graph stress versus strain for aluminum

APPENDIX C



Figure C: Graph stress versus strain for brass

APPENDIX D

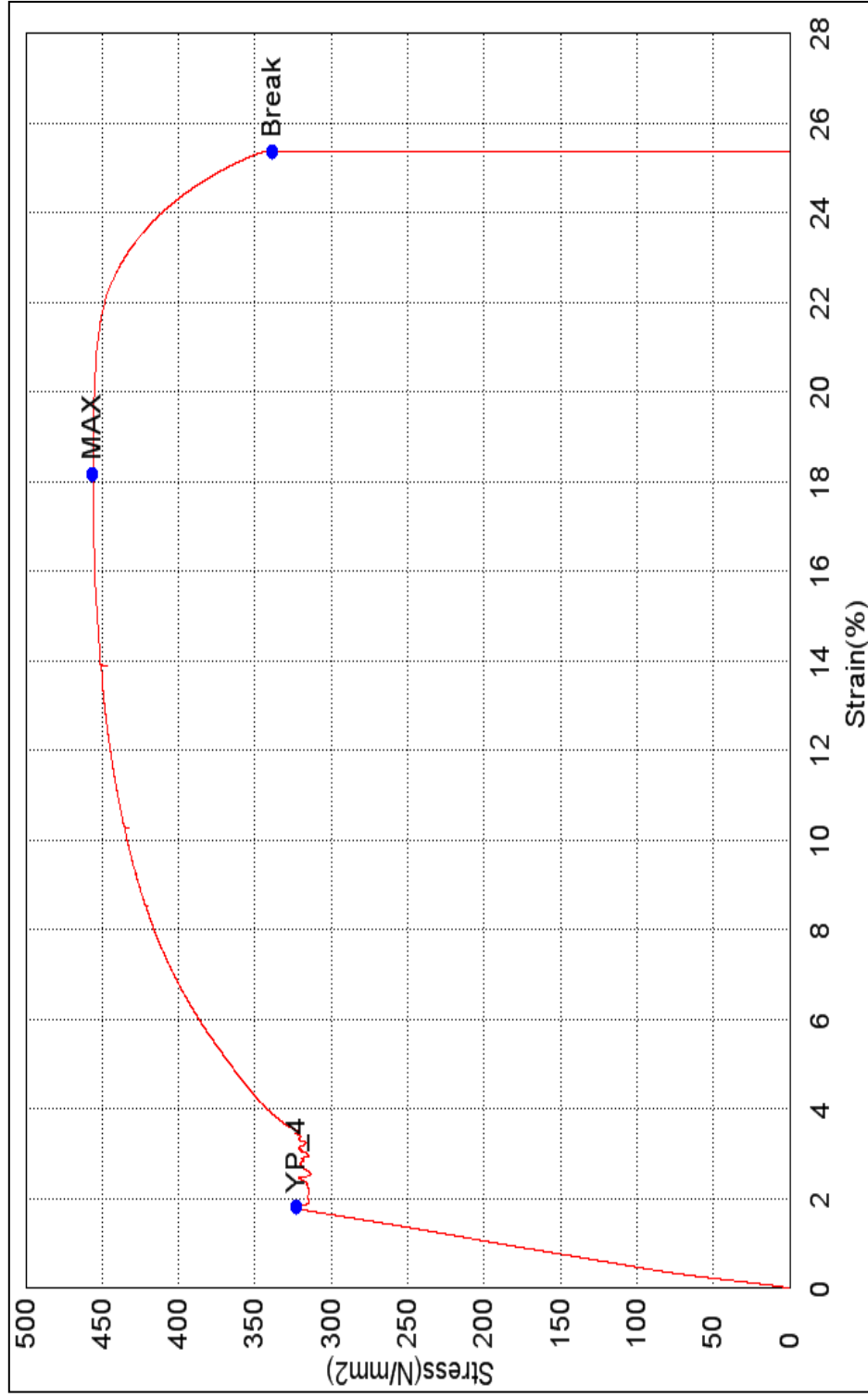


Figure D: Graph stress versus strain for mild steel

APPENDIX E

WEEK \ ACTIVITY	1	2	3	4	5	6	7	8	9	10	11	12	13	14	15
Briefing on title that I get from my supervisor	Yellow	Red													
Study about project and gather information		Yellow	Yellow	Yellow											
Prepare introduction		Red	Red	Red											
Prepare literature review						Yellow	Yellow		Red	Red	Red	Red			
Prepare methodology								Yellow	Red	Red	Red	Red			
Prepare specimen										Yellow	Red	Red	Red	Red	Red
Compile all data															
Complete the report											Yellow	Yellow	Yellow	Yellow	Yellow
Prepare presentation(slides)														Red	Red
Presentation														Yellow	Red

Figure E: Gantt chart for final year project 1

APPENDIX F

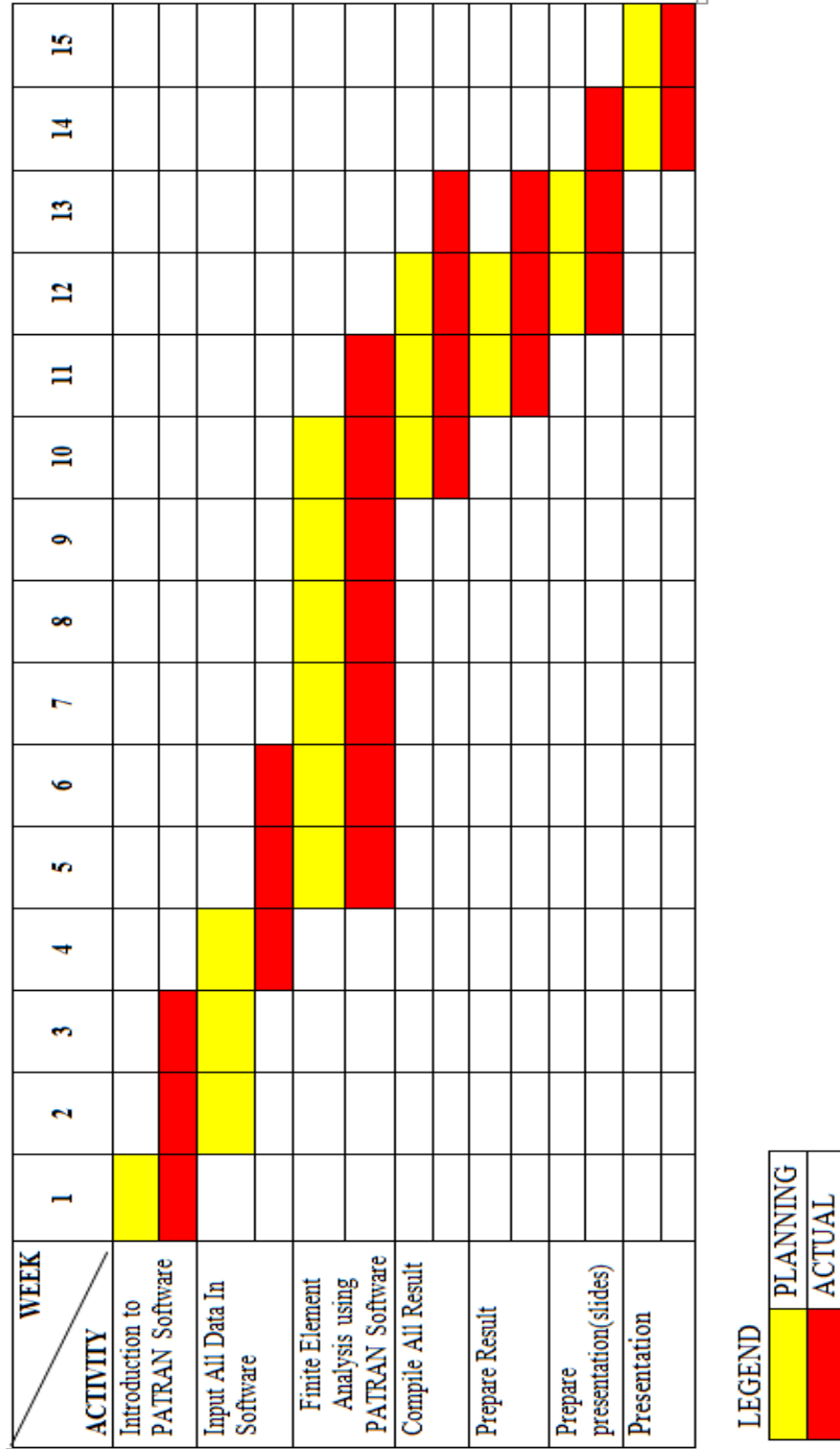


Figure F: Gantt chart for final year project 2